Håvard Fossum
Roman Pedersen
Stian Rasmussen

Bachelor's thesis

Modelling and optimisation of accumulator tank at NHL

May 2019

NTNU
Norwegian University of Science and Technology
Faculty of Engineering
Department of Energy and Process Engineering

NTNU
Norwegian University of
Science and Technology

Bachelor's thesis

2019

NTNU
Norwegian University of
Science and Technology

Håvard Fossum
Roman Pedersen
Stian Rasmussen

Modelling and optimisation of accumulator tank at NHL

Bachelor's thesis
May 2019

NTNU
Norwegian University of Science and Technology
Faculty of Engineering
Department of Energy and Process Engineering

NTNU
Norwegian University of
Science and Technology

NTNU

Faculty of Engineering

Department of Energy and Process Engineering

Bachelor thesis

Project title Modelling and optimisation of accumulator tank at NHL **Oppgavens tittel** Modellering og optimalisering av akkumulatortank på NHL-bygget	**Date provided** 09.11.2018 **Due date** 24.05.2019 **Number of pages in report / appendices** 60 / 18
Group participants Håvard Fossum Roman Pedersen Stian Rasmussen	**Supervisor** Kjell Kolsaker Associate Professor, NTNU kjell.kolsaker@ntnu.no 735 92 509
Study programme Renewable Energy	**Project number** FEN1909
Client NTNU Property Division	**Contact person** Christian Solli / 734 12 043

Free for publishing [X]

Temporarily nondisclosed [ ]

Free for publishing after [ ]

Preface

This bachelor's thesis is a part of the programme Renewable Energy at the Norwegian University of Science and Technology (NTNU), and concludes the three-year programme. It is the basis for assessment in the subject TFNE3001, and equates to 20 ECTS.

The thesis was provided by the Property Division at NTNU, and concerns itself with the simulation and analysis of a thermal energy storage tank at one of the campus buildings. It is written with the help of internal supervisor Associate Professor Kjell Kolsaker, and external supervisor Environmental Advisor at the Property Division, Christian Solli.

We would first and foremost like to thank Kjell Kolsaker for consistent and helpful meetings throughout the semester; this paper would not have been possible to write without him. We would also like to thank our external supervisor Chistian Solli for providing us with the thesis, as well as all the help he has given us.

Furthermore, the help and advice given by Staff Engineer at the Technical Management Section, Øystein Engan, have been invaluable, and a proper thank you is in order. Moreover, Senior Engineer at the Technical Management Section, Olav Høyem, contributed greatly by consulting and by giving us a review of the system.

Finally, we would like to thank Associate Professor Natasa Nord for her guidance with district heating; Assistant Professor and Vice Dean for engineering education at bachelor level, Audun Grøm, for his help with the economic analysis; Key account manager at Statkraft Varme AS, Terje Berg, for providing us with information on district heating tariffs; *Teknisk sjef* at Skala Fabrikk AS, Martin Sæterbø, for giving us information on the tank; and Senior Engineer at NTNU Campus Services Division, Trond Rikhard Haugen, for providing the investment costs of the system.

Trondheim, 24th May, 2019

Håvard Fossum

Håvard Fossum

Roman Pedersen

Roman Pedersen

Stian Rasmussen

Stian Rasmussen

Abstract

The objective of this bachelor's thesis is to create a model that simulates the reduction of thermal peaks of the district heat consumption by installing a $12m^3$ thermal energy storage (TES) tank to the local heating grid at *Norsk Hydroteknisk Laboratorium* (NHL). This is a pilot project considering reduction of energy consumption at Norwegian University of Science and Technology (NTNU), where the main goal is to evaluate how a strategy like this could help NTNU reach its short-term climate goals.

The model created for this thesis worked well, where it managed to shave the peaks adequately. It is appended to the document, and the usage here can be considered as a proof of concept. It can easily be adapted and applied in other scenarios if it is given more detailed input data than in this thesis, and it is perhaps best utilised if it is used in the planning phase of similar projects.

The model simulates the TES tank hour by hour, using historical data from 2017-2018. Case A utilises a deterministic and a genetic algorithm optimisation approach to shave the peaks as much as possible, where it analyses the heat consumption on a daily and a weekly basis for both methods. The results from the simulation are evaluated in regards to the Net Present Value (NPV), Payback Period (PP), and first-law efficiency. The weekly consideration cuts more of the peaks, and this is reflected by the fact that the NPV and PP were better for the weekly consideration than the daily. The worst peaks in the data set were cut from approximately 750kW to about 650kW in February 2018, the largest cut was around 175kW in May 2017, and the average reduction per month was 100kW. The NPV for the daily consideration was -775kNOK, while it was -768kNOK for the weekly consideration, and the PPs were 38 and 37 years respectively. The efficiencies were 96.3% and 88.8% for the daily and weekly consideration respectively. As the daily consideration had a better efficiency, and the difference in NPV amounted to 1.33%, it is therefore concluded that the daily consideration was the better strategy.

Case B compares different tank sizes, where $7m^3$, $10m^3$, $14m^3$, $17m^3$, and $22m^3$ were tested, to try to evaluate if a bigger tank would be better suited for the system at hand. Generally, the bigger tanks had better efficiency and lower PPs, as well as higher NPVs. The daily consideration had the better efficiencies, while the NPV and PP was better for the weekly consideration. The $17m^3$ and $22m^3$ tanks performed the best, however, due to the simplicity of the model utilised in the simulations, it is inconclusive whether these tanks are better suited for the system or not.

Sammendrag

Målet med denne bacheloroppgaven er å lage en modell som simulerer reduksjonen av termiske effekttopper i fjernvarmeforbruk ved å installere en 12m^3 akkumulatortank i sentralvarmesystemet i Norsk Hydroteknisk Laboratorium (NHL). Dette prosjektet er ansett som et pilotprosjekt for reduksjonen av energiforbruk ved Norges Teknisk-Naturvitenskapelige Universitet (NTNU), hvor målet er å evaluere hvordan en slik strategi kan hjelpe NTNU å nå sine kortsiktige klimamål.

Modellen som ble lagd under dette prosjektet fungerte på en god måte, hvor den tilstrekkelig klarte å kutte effekttoppene. Den er vedlagt dokumentet, og bruken av den i denne rapporten kan bli sett på som et ”proof of concept”. Modellen kan enkelt tilpasses og brukes i andre situasjoner dersom den mates med mer detaljert inndata enn som er brukt i denne rapporten, og er kanskje best egnet i planleggingsfasen av lignende prosjekter.

Modellen simulerer fjernvarmeforbruket ved NHL-bygget time for time for årene 2017-2018. Case A tar i bruk to optimaliseringsstrategier for å flytte lasten på en optimal måte; nemlig en deterministisk strategi og en genetisk algoritme. Simuleringene blir gjort der lasten ses på dag for dag og uke for uke. Resultatene blir evaluert med nåverdimetoden og tilbakebetalingsmetoden, og termisk virkningsgrad. De verste toppene i datasettet ble kuttet fra 750kW til 650kW i februar 2018, den høyeste toppen ble kuttet med ca. 175kW i mai 2017, og gjennomsnittlig kutt per måned i løpet av begge årene var 100kW. Nåverdien til investeringen ble henholdsvis -775kNOK og -768kNOK for daglige og ukentlige tilnærminger, med tilbakebetalingstider på henholdsvis nesten 38 og 37 år. Virkningsgradene var forholdsvis 96.3% og 88.8% for de daglige og ukentlige betraktningene. Virkningsgraden til de daglige simuleringene ble bedre enn for de ukentlige, og siden forskjellen i nåverdi var rundt 1.33%, ble den daglige betraktningsmåten derfor sett på som den mest optimale styringsstrategien.

Case B sammenligner ulike tankstørrelser, hvor 7m^3, 10m^3, 14m^3, 17m^3, og 22m^3 ble testet, hvor målet var å undersøke om en større tank ville vært et bedre alternativ i systemet. Generelt hadde de større tankene bedre virkningsgrad, høyere nåverdi, og lavere tilbakebetalingstid. Den daglige tilnærmingen hadde bedre virkningsgrad, mens den ukentlige tilnærmingen hadde bedre nåverdi og tilbakebetalingstid. 17m^3 og 22m^3 gjorde det best i simuleringene, men grunnet enkelheten ved modellen som ble brukt, er det derimot uvisst om disse tankene er bedre egnet til å stå i systemet eller ikke.

Nomenclature

Abbreviations

Abbreviation	Description
AN	Analytical solution to thermocline
BB	Black box solution to thermocline
CFD	Computational fluid dynamics
COP	Coefficient of performance
EPP	Evolutionary Progress Plot
ET	Energy temperature diagram
FM	Fully mixed tank model
GA	Genetic Algorithm
HVAC	Heating, ventilation, and air conditioning
LMTD	Logarithmic mean temperature
MB	Moving boundary model
MN	Multinodal model
NHL	Norsk Hydroteknisk Laboratorium
NPV	Net present value
PF	Plug flow model
PP	Payback period, used in economical analysis
TES	Thermal energy storage
ZN	Zonal model

List of symbols

Symbol	Unit	Description
A	m^2	Area
C, C_p	J/K	Heat capacity
c_p	J/(kg· K)	Specific heat capacity
$f(\mathbf{x})$		Objective function
F		Total fitness of population
$g(\mathbf{x})$		Inequality constraints
h	W/(m^2·K)	Heat transfer coefficient
$h(\mathbf{x})$		Equality constraints
k		Number of years in the NPV method
L	m	The length of a cylinder when calculating rate of heat transfer through the walls
M	kg	Mass of an object
m	h	Numbers of hours in period n
$\dot{M}$	kg/s	Mass flow rate
n		number of days/weeks in a year
p_c	%	Crossover rate
p_k, p_j		kth (or jth) selection probability in genetic algorithm
p_m	%	Mutation rate
Q	J, Wh	Heat energy
Q_{cons}	Wh/mo.	Heat energy consumed
Q_{tank}	kWh	Heat stored in the tank
$Q_{tank,max}$	kWh	Maximum heat stored on the tank. It is equal to 279.13kWh
$\dot{Q}$	W	Rate of heat transfer
$\dot{Q}_c$	W	Rate of heat flow due to convection
$\dot{Q}_{cond}$	W	Rate of heat flow due to conduction
$\dot{Q}_F$	kW	Heat bought from Statkraft Varme AS
$\dot{Q}_{F1}$	kW	Part of heat bought from Statkraft Varme AS delivered to the tank
$\dot{Q}_{F2}$	kW	Part of heat bought from Statkraft Varme AS delivered to the load
$\dot{Q}_{load}$	kW	Heat consumed by the building
$\dot{Q}_{loss}$	kW	Heat losses
$\dot{Q}_{max}$	W/mo.	Maximum power consumed over the period of one month
$\dot{Q}_S$	kW	The level at which the peak load should be shaved to
$\dot{Q}_{tr}$	W	Rate of heat transfer through a wall
$\dot{Q}_{VP}$	W	Power produced by heat pump
q_k		kth element in cumulative probability vector

R	W/K	The thermodynamic resistance of a body
r	m	Radius
r_g		Randomly generated number for selecting which gene is to be chosen for mutation
r_k		Randomly generated number for selecting which chromosomes to be chosen for crossover
r_{NPV}	%	Interest rate for the NPV method
r_o		Randomly generated number for selecting offspring
T	K	Temperature
T_i	K	Temperature difference on the hot inlet of heat exchanger
T_o	K	Temperature difference on the hot outlet of heat exchanger
T_S	K	Surface temperature of an object
T_∞	K	Ambient temperature
U	W/(m^2·K)	Overall heat transfer coefficient
v_k		kth chromosome in genetic algorithm
x		Vector element in input vector for the genetic algorithm
x_{tr}	m	Thickness of wall when calculating conduction heat transfer rate
$\mathbf{x}$		Input values of objective function, consists of $[x_1, x_2, ..., x_n]$
$\mathbf{x}^{\mathrm{L}}$		Lower bounds of input variables
$\mathbf{x}^{\mathrm{U}}$		Upper bounds of input variables
ΔT_{lm}	K	Logarithmic mean temperature
η	%	Efficiency of a system
κ	W/(m·K)	Thermal conductivity
Π	NOK	Price of district heating
Π_{diff}	NOK	The difference in price before and after peak shaving
Π_E	NOK/kW/mo.	Energy price
Π_P	NOK/kWh	Power price
Π_t	NOK	net cash inflow during year t in the NPV method
Π_{vol}	NOK/kWh	Volume price
ρ	kg/m^3	Density

Contents

List of Figures

List of Tables

1 Introduction

1.1 The scope of the project

The goal of this project is to simulate, analyse, and optimise the use of the thermal energy storage (TES) tank that is installed at the NHL building, at Campus Lerkendal-Valgrinda, in Trondheim. The tank is installed in the system to shave large power peaks to both reduce the costs, as well as to increase the self-sufficiency regarding energy, and use the energy more efficiently. The model is to be built in MATLAB, and will be based on historical data that spans the years 2017-2018.

The project will be divided into two cases, A and B. Case A will evaluate the tank that is installed in the system, and it will try to ascertain a strategy for when to charge and discharge the tank. It will further be divided into two parts, where case A1 and A2 will utilise two different optimisation strategies to do this. The strategies in question are firstly a classical optimisation strategy, while the second is a genetic algorithm approach. Case B will try to evaluate how different tank sizes would perform in the system, and it will try to find an optimal tank size based on the energy efficiency, the costs of the tank, and the savings generated from peak shaving.

This paper will be divided into seven chapters; namely the introduction, a theory chapter, method, results, discussion, conclusion, and future work. The theory chapter concern itself with presenting relevant theory on thermodynamics, accumulator tanks, heat pumps and heat exchangers, district heating, optimisation strategies, and economic analysis. The method chapter describes the methods used and components evaluated in detail, and formulates the cases A and B. The results from the simulations are then presented in the results chapter, and scrutinised in the discussion chapter. A final chapter presents the possibilities of future work around the tank, and around the system as a whole.

1.2 NTNU Climate Goals

In light of climate change, NTNU has devised an action plan to reduce their own climate footprint. The current action plan was to last from 2011-2020 [1], but a new plan that is more ambitious is in the works for the period 2019-2030 [2]. In the plan for 2011-2020, one key part is that the energy consumption shall be reduced by 20% compared to 2010. The second goal concerns NTNU's buildings, where 5% of them shall be rated A [1]. To achieve these goals, the following measures can be taken: they can reduce the amount of energy they consume; change the operations of their facilities; change the use patterns of their buildings; and by new investments to upgrade their buildings to newer building standards in regards to energy efficiency [1]. As part of the state budget in 2017, the Norwegian government requested that NTNU's new campus should be developed with ambitious climate goals, and NTNU has since then been granted funds from Enova to conduct a survey that tries to ascertain where energy consumption can be reduced, where they can produce their own energy, and if it is possible to store the energy. It is presumed that this will reduce the total amount of energy they consume, which will reduce the energy costs, and will also reduce the strain on the infrastructure that delivers the energy [3].

NTNU would like to be the leading university who uses the internal research to become an overall environmentally responsible institution. In addition, NTNU want to gain an overview of environmental impact that the institution has, and to showcase it for employees, students, and the society. At all stages NTNU will have a dedicated goal for how the environmental impact would be reduced [2].

NTNU's climate goals are the background for this thesis. An analysis of the central heating system at NHL will work as a small-scale pilot project regarding thermal energy storage and production at campus, and this thesis will try to contribute in this regard.

2 Theory

2.1 Thermodynamics

A selection of relevant thermodynamic principles will be presented in the following section.

2.1.1 Thermodynamic concepts

A useful thermodynamic concept is enthalpy, which, under certain conditions, describe the heat within a system. Enthalpy is dependent on the properties temperature and pressure. For incompressible substances, internal energy, volume, and enthalpy, may be evaluated only with consideration of temperature, as they change negligibly little with changes in pressure. Heat capacity C is a property that, under certain conditions, relate the change in temperature to the amount of energy added or subtracted by heat transfer to a system. Heat capacity can be described with either internal energy or enthalpy in mind, where it is denoted as and C_p if it is considered in regards to enthalpy. These two heat capacities are equal for incompressible substances [4].

2.1.2 The first and second law of thermodynamics

The first law of thermodynamics states that the total amount of energy within a system must be conserved; energy can neither be created nor destroyed, only change form [4]. With this in mind, the first-law efficiency can be defined – it describes the the thermal efficiency concerning charging, discharging, and storing of thermal energy, and accounts for the thermal losses in this process [5].

To define the second law of thermodynamics, different statements must first be presented [4].

The Kelvin-Planck statement says that a system cannot perform in a way where it is receiving heat from only one single thermal reservoir and turning all of the heat into work. A consequence of this statement is that a thermodynamic cycle never can achieve a thermal efficiency of 100% [4].

The Clausis statment defines that heat is limited to be transferred from the warm to the cold reservoir if the system is limited to two reservoirs. This means that without an external force, heat cannot be transferred from a cold to a hot body. However, if there is some external force, it is possible to do so [4].

Another statement concerns itself with entropy. Entropy represents the loss of useful energy. It states that entropy can never be destroyed; entropy can only be transferred and created [4].

The second law and its deduction have some useful applications when working with for example a heating or cooling system. The direction of a cycle is determined by the second law, which may be useful when trying to understand and create a heat cycle. It may also be used to learn about the equilibrium of the system as well as to find the maximal thermal efficiency. Furthermore can the required temperatures be scaled by the help of entropy [6].

Entropy is also used to define exergy. Exergy is the energy that can be used to perform work [4]. This gives rise to the concept of second-law efficiency. This efficiency, applied to TES, describes the degradation of the energy stored, due to the temperature difference in the charging and discharging process, as well as the heat losses. It also accounts for exergy loss in heat exchangers [5].

2.2 Heat transfer

Heat transfer is a physical form of exchanging thermal energy in a medium or between media, where temperature and heat flow are the main principles of heat transfer [7].

There are three methods of heat transfer, namely *conduction*, *convection*, and *radiation*. Radiation and conduction are only dependent on the temperature difference. Convection, on the other hand, is dependent on mass transport of fluid and the temperature difference. In addition, all have the capability to transfer heat through materials, while only radiation has the capability to transfer heat through vacuum. All of these methods transfer energy from high to low temperature regions [8].

2.2.1 Conduction

Heat transfer in form of conduction happens by molecular motion where the energy is transmitted between the interconnected areas. The transfer of energy will occur when one of the areas has higher temperature than the other, and the energy will move from the high to the low temperature area. The higher temperature area will contain molecules which are more energetic, and the area with the lower temperature will contain less energetic molecules. When there is an interconnection between two areas with different temperatures the molecules will collide, and the energy will transfer from the molecules that are more energetic to the molecules that are less energetic. The movement of the energy that occurs in conduction must transpire in the same direction as decreasing temperature [6, 8].

The equation that describe this rate of change for conduction derives from Fourier's law of heat conduction, and is shown in equation (2.1). This equation is the definition of thermal conductivity, where it describes the transmission of heat trough a particular substance:

$$\dot{Q}_{cond} = -\kappa A \frac{\partial T}{\partial x_{tr}} \tag{2.1}$$

In equation (2.1), $\dot{Q}_{cond}$ represent the rate of heat flow from the surface area, κ is a constant which represent the materials conductivity as a heat flow per unit time per unit area, A is the surface area that the heat flows out from, and $\partial T/\partial x_{tr}$ represent the temperature difference between two areas and the distance of the heat transportation [6, 7].

2.2.2 Convection

Convection is a form of heat transfer where the thermal energy is usually transported between a fluid that flows along a solid and the solid object itself. The principle for heat transfer is the same for both conduction and convection, however, convection accounts for fluid in motion, while conduction does not. Convection will therefore have a similar physical interaction between molecules as conduction [7, 8].

When the process that includes the fluid motion has external means of affecting the heat transfer, then the process would be called *forced convection*. The external means could refer to a pump, wind, or a ventilator. If the process has fluid motion which derives from external force fields, such as gravity, which will have an effect on the density gradient induced by the process itself, then it would be called *free convection*. A mix of both *free* and *forced convection* effects in a system would be called *mixed convection*, however, this requires that both of the effects are noteworthy and neither one of them can be neglected [7, 8].

The rate of change of convection can be described by equation (2.2); it is also known as Newton's law of cooling when a fluid is used to cool down a solid surface.

$$\dot{Q}_c = hA(T_s - T_\infty) \tag{2.2}$$

In the above equation, $\dot{Q}_c$ is the rate of heat flow for convection, h represents heat transfer coefficient of the material, A is the area surface where the heat is transmitted from for the solid material, $(T_s - T_\infty)$ is the temperature difference between the solid surface and the fluid that describe how much heat is transported away [7, 8].

2.2.3 Radiation

In contrast to the other two heat transfer methods, radiation transmits heat in a form of electromagnetic waves around the infrared zone. Radiation of the electromagnetic waves occurs at every temperature except absolute zero, and the object that radiate the energy do it in all directions. The temperature plays a important role as an increment in temperature will also increase the amount of energy that is radiated. The energy that is radiated can impact other objects, where part of the energy may be reflected, part of it may be absorbed, and another part may be transmitted past the object. If two objects with different temperatures are in proximity of each others radiation, the object that has the lowest temperature will receive more energy than what it radiates, and therefore have an increment of internal energy [6, 7].

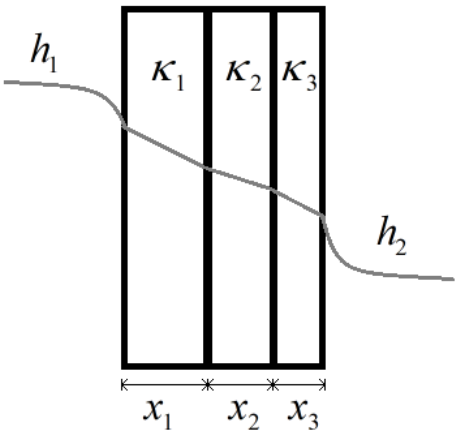

Figure 1: Sketch depicting heat transfer through composite wall. The grey line indicates the heat transfer.

2.2.4 Heat transfer through a wall

In complex situations, more than one of the modes of heat transfer may occur at the same time. This is also true for heat transfer through composite walls, where each layer leads heat differently. Energy transfer through a composite wall is depicted in figure 1. When evaluating heat losses through a composite wall, the heat transfer is evaluated by the equation

$$\dot{Q}_{tr} = \frac{\Delta T}{\Sigma R} \tag{2.3}$$

where ΔT is the difference in temperature on the outside and the inside of the tank, and ΣR is the thermodynamic resistance through the wall, and is dependent on, among other things, the material(s) used. ΣR for a composite wall can be found by:

$$\Sigma R = \sum_{i=1}^{n} \frac{1}{h_i A} + \sum_{j=1}^{m} \frac{x_{tr,j}}{\kappa_j A} \tag{2.4}$$

where A is the area, h_i is the ith heat transfer coefficient, which is evaluated at the ends of the wall, and represents the convection component; and κ_j is the the thermal conductivity of the jth layer of the composite wall, the sum of which represents the conductivity component [9].

When evaluating heat transfer through a cylinder (e.g. through a TES tank), ΣR is found by

$$\Sigma R = \sum_{i=1}^{n} \frac{1}{h_i 2\pi r_i L} + \sum_{j=1}^{m} \frac{\ln(r_j/r_{j-1})}{2\pi L \kappa_j} \tag{2.5}$$

where L is the length of the cylinder, and together with $2\pi r_i$ constitutes the cross sectional area of the cylinder in the ith layer. Both equations (2.4) and (2.5) are derived from equation (2.1) and (2.2) [9].

2.3 Thermal energy storage

TES is the storage of heat energy, in order to be able to use it at a later time. Two main forms of TES exist, namely latent and sensible energy storage. Latent TES is the storage of thermal energy as a phase change at constant temperature, while sensible TES is the storage of thermal energy by elevating the temperature of a substance [6]. In this report, latent heat storage will not be discussed further.

2.3.1 Sensible TES

Sensible heat generally utilises water as the storage medium. It has some of the highest specific heats of any liquid at ambient temperatures, and, although solids have larger specific heat capacities, water is a liquid, which makes it easier when transporting the heat. In addition, water also has good heat transfer rates [6].

Diurnal TES is the storage of heat where the cycle of charge and discharge happens over the course of a day. This is in contrast to seasonal or annual TES, where the heat charge/discharge cycle happens during the course of months. Diurnal TES can be used for load management, where thermal energy can be stored when the demand and prices are low, and the energy can be released when the demand and prices are high. This also leads to the

serendipitous effect of causing less strain on the electric grid, if electrical heating is used [6]. These same principles can be applied to district heating as well.

To store sensible heat, a container, a storage medium, as well as an input/output device is needed. It is also necessary that the container negates heat losses. The amount energy is stored within a medium is given by the equation:

$$Q = Mc_p\Delta T \tag{2.6}$$

where Q is the amount of heat energy is stored in a body of mass M and a specific heat capacity c_p, given that the temperature increase with an amount equal to ΔT [6]. The power can be evaluated if Q is differentiated in respect to time, so that

$$\frac{\mathrm{d}Q}{\mathrm{d}t} = \frac{\mathrm{d}}{\mathrm{d}t}\left(mc_p\Delta T\right) \Rightarrow \dot{Q} = \dot{M}c_p\frac{\mathrm{d}(\Delta T)}{\mathrm{d}t} \tag{2.7}$$

where $\dot{M}$ is equal to the mass flow rate through the boundaries of the system. The term $\mathrm{d}(\Delta T)/\mathrm{d}t$ represent the change in the temperature difference over time.

2.3.2 Storage tanks and stratification

Stratification is an effect often found in heat storage units. When water is heated, the density changes, leading to the colder water sinking to the bottom of the tank, while simultaneously the hotter rising to the top. According to Dincer and Rosen [6], a TES tank can be considered as having two zones at different temperatures, as well as one with mixed temperatures in the middle. The mixed temperature zone is called the thermocline, and the temperature distribution here follows a gradient between the low and the high temperature regions, as illustrated in figure 2. The degree of stratification is measured as how thick the thermocline region is, where highly stratified tanks have a narrow thermocline and vice versa [10].

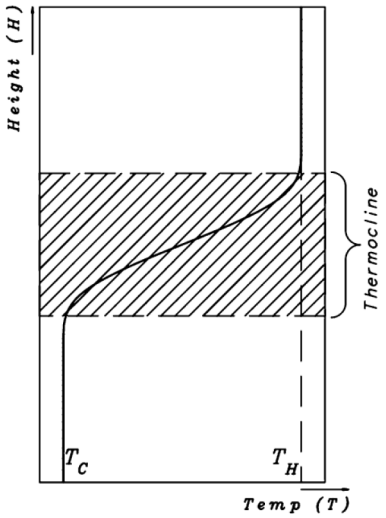

Figure 2: Illustration of a thermocline region, and temperature gradient. From [10, Fig. 1].

Different factors, for example the size and design of the tank, are affecting the state of the stratification in the unit. According to Zheng et al., tanks with sharp corners – i.e. cones, cylinders with cone, and spindle shaped tanks – has the highest stratification, while a tank with horizontal plane surfaces – i.e. circular truncated cones, barrels, cylinder with truncated cone, and cylinders – has the lowest stratification [11]. Furthermore, the inlet and outlet stream will mix the water, which is the most important factor causing stratification to be lost. Heat losses to the surroundings, heat conduction between the different layers in the unit and convection in the walls also affect the

stratification [6]. A phenomenon known as quilting, which is "[...] heat loss due to recirculation of water in the tank from hydraulic connections" [12, p. 3], will also affect the performance of the tank.

The main consequence of loss of stratification is loss in efficiency. According to equation (2.6), a greater ΔT will lead to a greater amount of energy to be present. This causes there to be more energy stored in the tank if a temperature gradient is present between the top and bottom. This ultimately leads to a considerable increase in efficiency if the tank is stratified [6].

2.3.3 Mathematical modelling of TES tanks

There are several ways to model a TES tank. Dumont et al. [12] proposes a classification to group the different types of models into eight different classes:

1. Analytical (AN): It utilises Laplace-transformations and several simplifications to attain an analytical solution to how the thermocline develops during charging and discharging;
2. Fully mixed (FM): It assumes a fully mixed tank, and simplifies the problem in such a way so as to be evaluated by only the the inertia of the fluid, the heat input and output, and the ambient losses to the surroundings;
3. Blackbox (BB): This class of methods utilises neural networks to simulate the tank;
4. Two zone moving boundary layer (MB): This model is similar to the fully mixed model, but with two zones that are fully mixed rather than one, which are divided by a perfect infinitesimal thermocline. The hot volume represents the energy stored in the tank. It does not consider heat or mass transfer between the fluids;
5. Plug flow (PF): This model consists of n isothermal volumes that move throughout the tank, where no mixing between the layers occur. A variable inlet is often used, so that a rising temperature gradient is to be located inside the tank;
6. Multi-node (MN): These models assume uniform temperatures horizontally, and a one dimensional flow. It then solves energy balance equations for each node, which also takes into account losses due to buoyancy and other disturbances;
7. Zonal (ZN): This model utilises a large mesh grid where energy balance equations are verified, but does not take into account momentum conservation. It takes complex fluid disturbances into account; and
8. Computational fluid dynamics (CFD): This method uses a mesh grid where the Navier-Stokes equations are applied with conservations of mass, energy, and momentum, for each mesh volume. It can be modelled either two- or three dimensionally.

A figure depicting some of the methods mentioned above are presented in figure 3. Each of the models mentioned above have their associated strengths and weaknesses, where they may sacrifice accuracy for quickness of computation, or vice versa [12].

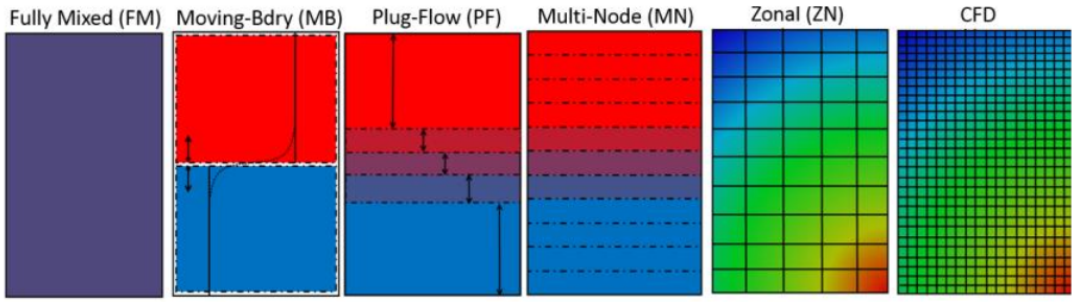

Figure 3: Sketches depicting the different tank model classes proposed by Dumont et al. Figure from [12, Figure 2].

2.3.4 TES tank performance and volume optimisation

TES tanks can often improve the overall performance of a system significantly. However, it causes the system and control strategies to be more complex, and it adds additional investment costs to the system. Determining the right shape and size of the tank depends on what is desired from the TES tank, as it can affect both the costs and the efficiency. For instance, spherical and barrel shaped tanks have the best thermal energy capacities, while cylindrical tanks has the worst thermal energy capacity. Zheng et al. also states that cylindrical shapes has the worst thermal efficiencies, while the spherical ones has the best efficiencies [11]. The size of the tank is an especially important aspect when designing the system, as if it is too large, the increased costs and heat losses negate the added benefits of the tank, especially for larger buildings [13]. A too small tank will not be able to shave the peaks sufficiently.

A standard way to determine the tank size does not currently exist. According to Wang et al., the current guidelines to determine the tank size are based upon field experience and rules of thumb [13]. Typically, an early stage assessment of TES tank size can be determined by conducting an economical analysis. However, this will yield inaccurate results, and the performance of the tank is needed to be assessed to confidently determine if the selected size is adequate or not. Ma et al. proposes a method where the storage effectiveness, the first-law and second-law efficiencies are used to determine an optimal size of the tank. The effectiveness in TES is the usable volume of the unit, and it is determined to be the areas above and below the thermocline region [5].

There are several ways to determine the efficiency of a TES tank, and currently, there are no standard way of comparing and evaluating TES tanks. Dinçer & Rosen [6] presents several ways to calculate the efficiency, in terms of both energy and exergy. They all account for energy input, energy output, the initial and final state of the energy, and the temperatures at which the heat transfers occur. Four efficiencies are described for each of the charging, storing, discharging, and overall processes, where they can be either calculated in terms of energy or exergy. The exergy efficiencies are more meaningful, as the energy efficiencies does not consider the temperatures of the energies – as Dincer & Rosen puts it:

> Examining energy efficiencies alone can result in misleading conclusions because such efficiencies weight all thermal energy equally. Exergy efficiencies acknowledge that the usefulness of thermal energy depends on its quality, which is related to its temperature level [6, p. 269].

Furthermore, the different efficiencies are better to use in some scenarios than others. However, for complete charge, store, and discharge cycles, all the efficiencies are both valid and useful. One of the proposed overall efficiencies will be used in this report, and it is defined as:

$$\eta = \frac{\text{Energy recovered + final energy in store}}{\text{Energy input + initial energy in store}} \tag{2.8}$$

The energy recovered indicates the energy discharged from the unit. This entails that the efficiency is equal to one if the storage is adiabatic, while it is equal to zero if the initial energy in store is equal to the final energy in store [6]. The second-law efficiency will not be evaluated in this report.

2.4 Heat pumps

A heat pump takes high value energy, mainly electrical, and mixes it with lower value energy such as thermal, and increases the value of the energy. This fact makes it one of the most efficient ways for heating, in terms of both costs and energy. The coefficient of performance (*COP*) is the relation between the heat leaving and the electric energy added to the heat pump [14].

A typical air/water heat pump operates with exhaust air from the ventilation or with outdoor air, and the energy that is extracted is used for heating an area or a hot water system. Thermal performance for a heat pump can vary from only a few kilowatts for the smallest systems and up to 100kW for larger systems, all dependent on what environment the heat pumps are used in. The working medium in an air/water heat pumps usually consist of R-22, R-404A, R-407C, R-134a or propane. For temperatures higher than 60/65°C in the hot water system, propane is commonly used as the working medium in the heat pump [14].

Outdoor air is easily accessible everywhere, which makes it a very useful heat source, and it has a lot potential for use in heat pumps. Two disadvantages with air as the heat source, would be the low heat transfer property and its density. To avoid big heat transfer surfaces, it would require a sizeable temperature difference between air and the working media, in addition to extensive circulation of air. These circumstances contribute to rise in electrical energy consumption. Air heat pumps are therefore most optimal in environments where the temperature will not sink too low, and where the temperature remains relatively uniform throughout the year [14].

Low outdoor temperatures will have a negative impact on the coefficient of performance, which may impact the profitability of running the heat pump. Heat pumps deliver the least heat when the demand for heating is at its highest, and vice versa. The days with the lowest temperatures may even need to be completely covered by the peak load machines, as extremely low outdoor temperatures may cause damage to the heat pump [14]. At temperatures below 0°C, it becomes necessary to de-ice the heat pump, which requires more energy than would normally be needed to run the machine [15].

2.5 Heat exchangers

A heat exchanger is used to transfer heat from one medium to another. This process may occur in different ways; either by media being in direct contact with each other or with a border to prevent them from reacting or mixing [16]. When the media are at different temperatures, heat is transferred between them. This follows the second law of thermodynamics, where the energy in the form of heat transfers from the warmer to the colder area. One of the main benefits of separating the flows, is that it is possible to sustain different pressures, temperatures, and chemical compositions [7]. When dealing with a wall, equation (2.2) is a suitable way to calculate the heat transfer.

However, when calculating the heat transfer through a heat exchanger, the logarithmic mean temperature, $LMTD$, is introduced.

$$Q = UA\Delta T_{lm} \tag{2.9}$$

where

$$\Delta T_{lm} = \frac{T_i - T_o}{\ln(T_i) - \ln(T_o)} \tag{2.10}$$

T_i is the difference in temperature on one side of the heat exchanger and T_o is on the other. This equation is used for cocurrent and countercurrent flows [7]. As seen in equation (2.9), the heat transferred through a heat exchanger is dependent on area and thermal conductivity of the exchanger itself, as well as the temperatures of the media entering the exchanger. The temperatures of a system is commonly predetermined, making the area the only way to change the capacity of the heat exchanger. To increase its area, fins are often used. A fin can be a thin extension to efficiently increase the area of a heat exchanger [7]. Figure 4 shows how fins may be attached to a pipe to increase the area and thus also the heat transfer rate. It is important to note that an undersized heat exchanger will be unable to transfer the necessary heat, while a an oversized one will increase the investment costs [17].

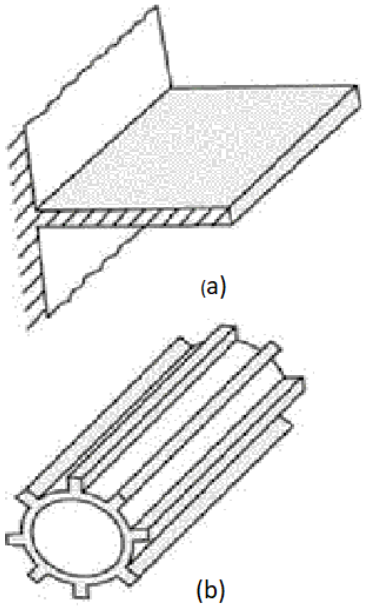

Figure 4: Different fins used for heat exchangers, showing two figures from [7, Fig. 2.30 a and e]. (a) is showing a thin plate fin and (b) is showing how a fin may look attached to a pipe.

One way of categorising heat exchangers is by the direction of the flow. The four most important are cocurrent, countercurrent, single-pass and multi-pass crossflows. From these, the counterflow is the most efficient in terms of heat transferred by area [7].

2.6 Heat distribution

2.6.1 District heating

District heating is a heating system where several buildings and residences receive heating from a centralised heating facility. The heat is transported by water in pipelines, with a hot supply pipe, and a cold return pipe, where the consumer is most commonly connected to the grid via heat exchangers. There are three main components in a district heating network, namely a centralised heat source, a transmission network, and substations. The centralised heat source is the facility that heats the water, the distribution network is the network that distributes the heat to the consumers, while the substations are the interconnections between the network and the consumer [18, 19].

In Trondheim, the district heating network is operated by Statkraft Varme AS. They divide their heating networks into two layers: The primary network is a network directly linked to their heating stations, while the secondary network is a network mainly used in connection to residential areas, and will thus not be discussed in this report. These network layers operate at different temperatures and pressures, and are hydraulically isolated from each other. Normal operating conditions on the primary network is supply temperatures between 80 and 110°C (but can be as high as 120°C some places at certain times), at pressures ranging from 0.5-2.0 MPa, depending on the geographic position and times of year, while the minimum supply and return temperature difference is 50°C [21]. The heat sources used by Statkraft Varme AS are mainly heat generated from incineration of waste, but they also utilise biogas and ocean heat pumps, but other sources are also used to cover peak and intermediate loads, as depicted in figure 5 [22].

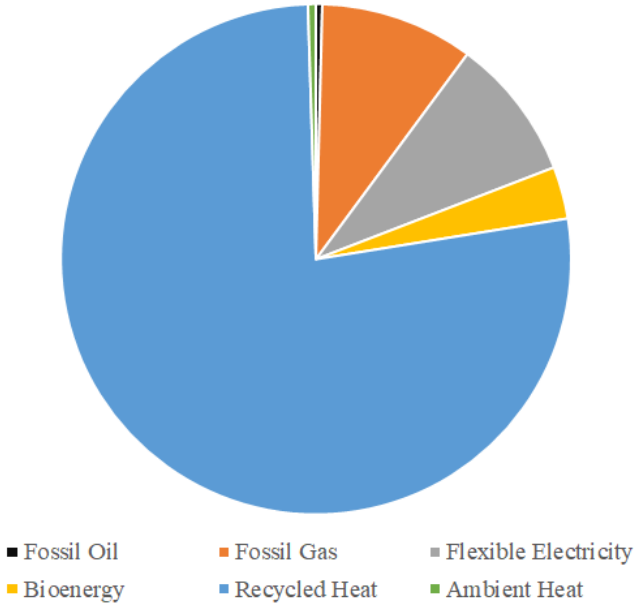

Figure 5: A pie chart that showing the heat sources used in Trondheim in 2017. Data from [20].

2.6.2 Load management

District heating grids often face large variation in loads during the day. Loads are classified into three distinct groups, namely base load, intermediate load, and peak load. Base load covers the largest part of the heating loads, and is often more environmentally friendly. The intermediate load units are generally more costly than the base load, while the peak load units are often small, and only run for a limited time during the day. They are the most expensive units, and they often use fossil fuels, but they are needed when the base and intermediate load units does not suffice. The different load types are shown in figure 6 [23]. It was mentioned in chapter 2.3.1 that energy storage could be used for load management. This usually means that the peak load is moved from the day to periods with

low demand, where the loads are generally much lower [24], and thus shaving the peaks. This principle is true for central and district heating alike. NTNU Property Division assumes a flat 200g CO_2/kWh for both electricity and district heating [2].

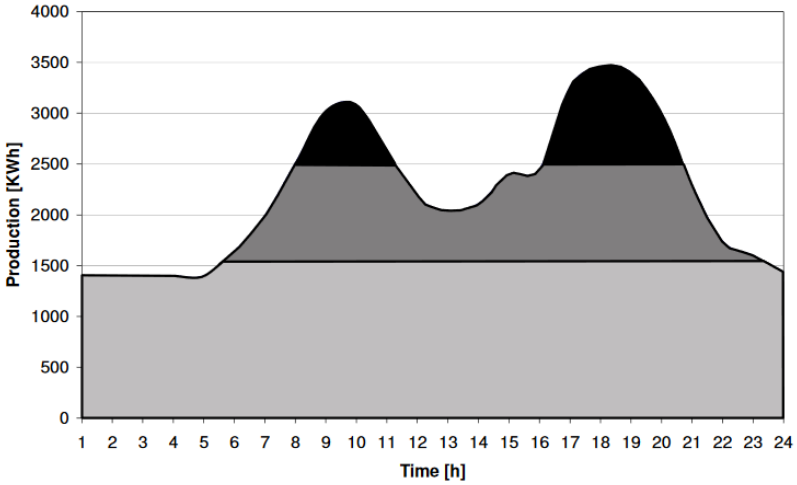

Figure 6: An illustration of the different load types. The bottom part is the base load, and the section at the top is the peak load, while the section in-between is the intermediate load. Figure from [23, Fig. 4]

There are several methods that can be used to evaluate the loads of a heating network. One useful tool is the duration curve. This curve is evaluated for a specified duration, and it displays for how long a specific power level is used, as shown in figure 7 [25]. The far left region of the curve represents the peak load, and is useful for e.g. designing how large the portion covered by base load is, and thus how large peak load units have to be to cover the total load of the building throughout the year [14].

Another useful tool is the energy temperature curve (ET curve). This plots the mean outdoor temperature on the x-axis against the energy consumption on the y-axis, where the energy data should ideally align itself linearly as the temperature increase. This tool is useful to investigate where the energy consumption is larger or smaller than what should be expected at a certain temperature, and large variations or spread indicates a bad control strategy or a faulty facility [14, 25].

2.6.3 Central heating

A central heating system is the system that delivers heat internally to a building. A water central heating system consists of pipes, pumps, valves, energy central, and heating elements. Norwegian systems have generally used a two-pipe system, where the supply and return pipes are coupled in parallel over the radiators. The main functions of the energy central is a system for heat absorption (heat source/sink), heat production (e.g. through heat pumps or peak load units), and heat distribution trough pumps, fans, etc. [14].

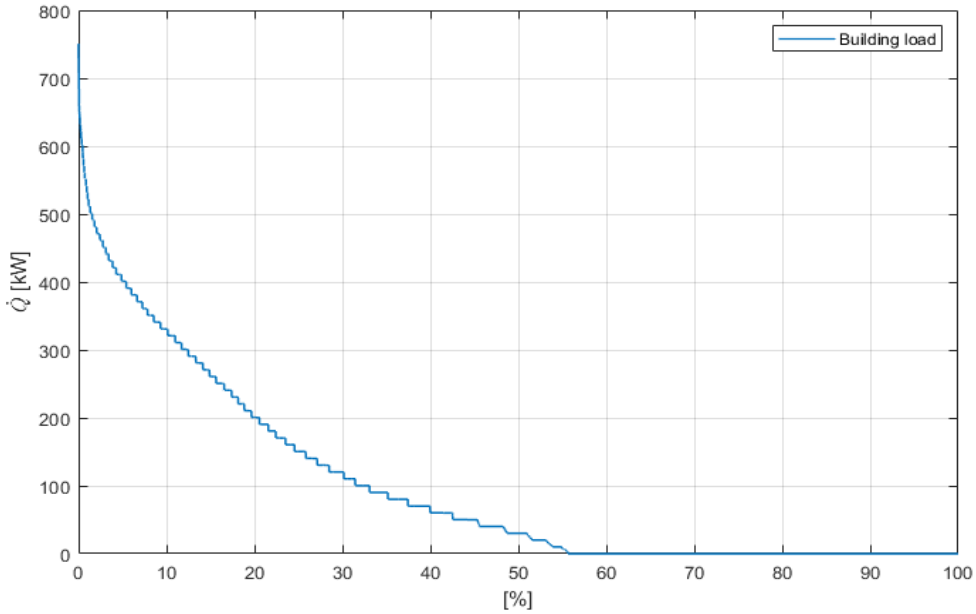

[H]

Figure 7: The duration curve of the load at NHL in the period 01.01.2017 and 31.12.2018, made from the data set supplied by NTNU. Data arranged and plotted with [26].

There are several ways to distribute heat through a central heating system. Different temperature schemes exists, where typical high-temperature heating systems deliver water at 80°C, and the return water is typically at 60°C, while low-temperature heating systems typically supply and return water at 55°C/45°C. The systems work in such a way that heated water from the energy central is distributed to different sections (called secondary circuits) through a distribution manifold, where the heat is dissipated through heating elements (such as radiators), and the water is then transported back to the energy central through a collector manifold, where it is reheated. The energy central along with the manifolds are called the primary circuit [14].

Central heating systems in Norway are generally divided into two systems when it comes to regulating heat flow, and the two systems are:

1. Constant fluid flow rate in the secondary circuits, independent on the specific heating needs at that particular time. This type is thus temperature regulated.

2. Varying fluid flow in the secondary circuits, where the flow is dependent on the specific heating needs at that particular time [14].

However, real systems may be regulated by a combination of temperature flow rate regulation – for instance, the temperature in flow rate regulated systems are often compensated for by the outdoor temperature to be better suited to different scenarios other than the design scenario [27].

2.7 Optimisation

Optimisation is a field in mathematics concerning itself with finding minima or optima of a function, given a single or a set of input(s), while also satisfying one or more constraint(s). The function in question is generally called an objective function. Several strategies exist to solve an optimisation problem, and different strategies may be more feasible to use depending on the problem at hand. A typical engineering optimisation problem is expressed as a minimisation or maximisation of a function, subject to inequality and/or equality constraints. It may be formally presented as:

$$\begin{array}{lll} \text{Minimise} & f(\mathbf{x}) & \\ \text{subject to} & g_i(\mathbf{x}) \leq 0 & \text{where } i = 1,2,...,m \\ \text{and} & h_j(\mathbf{x}) = 0 & \text{where } j = 1,2,...,\ell \\ \text{and} & \mathbf{x}^{\mathrm{L}} \leq \mathbf{x} \leq \mathbf{x}^{\mathrm{U}} & \end{array}$$

where $\mathbf{x}=[x_1, x_2, ..., x_n]^{\mathrm{T}}$, and represent n real inputs or design variables. g_i are inequality constraints, while h_j are equality constraints. $\mathbf{x}^{\mathrm{L}}$ is the lower bound of the design variables, while $\mathbf{x}^{\mathrm{U}}$ is the upper bound (which are also considered inequality constraints). A solution to the problem which satisfies the constraints is called a feasible solution (and all feasible solutions are called the feasible region) [28].

2.7.1 Optimisation techniques and genetic algorithms

All optimisation problems follow a sequence of steps, which asymptotically converge towards an optimal solution. Conventional optimisation techniques generally utilise a deterministic algorithm where gradients or higher order derivatives of the objective function, at a single point, are used to determine which direction to explore between each iteration. One of the main problems with this approach, is that the algorithm does not leave any room to explore other parts of the feasible region, and thus run the risk of finding local optima or minima, rather than a global one [29].

Another approach to solve optimisation problems, are genetic algorithms (GAs), which is a type of evolutionary algorithm. These techniques emulate evolution to explore the feasible region, and rather than using a point-to-point exploration, it utilises a set of solutions, and uses probabilistic transition rules between each iteration to develop the most promising regions further [29].

According to Gen & Cheng [29], there are several major advantages to genetic algorithms when compared to its classical counterparts. Firstly, as mentioned above, they (probabilistically) negate falling into local optima or minima due to their global search nature; secondly, no advanced or complicated mathematical knowledge is a prerequisite to use a GA; and lastly, they will search for solutions without regard to the inner workings of the problem at hand [29].

A genetic algorithm starts with a random input, called a population. Each element in the population is called a chromosome, all of which represent a feasible solution to the problem. The chromosomes are usually encoded as binary strings. The population evolves through each iteration, which is called a generation. Each chromosome

will be evaluated by a cost function at each generation, the best of which are selected to be the basis of the new population, called the offspring. This is done by either a crossing of two chromosomes to form a new one, or by mutating a chromosome, or a combination of both. The chromosomes that score badly on the cost function are discarded, so as to keep the population size constant. Which chromosomes to be crossed are determined by the crossover rate p_c, where a larger rate will result in a larger part of the feasible region to be explored. This rate is defined as the number of offspring produced divided by the population size. The mutation rate p_m determines how many genes are mutated at each generation, and is defined as a percentage of the total number of genes in the population. A gene is a single bit in the bit string representation. An encoded (i.e. a bit string representation) chromosome is called a genotype, while the decoded (i.e. decimal representation) chromosome is called a phenotype [29].

If the optimisation problem is defined, a simple GA can be constructed as follows:

Step 1

The design variables must be encoded into binary strings, the length of which is determined by the needed accuracy [29].

Step 2

The initial population must be generated [29].

Step 3

The chromosomes must be evaluated, and the fitness must be determined. For maximisation problems, the fitness may be defined as equal to the value of the objective function [29].

Step 4

The next step is selection. A widespread approach is the roulette wheel approach, which will be described here. After the fitness value is calculated, the total fitness of the population must be found. This is found by:

$$F = \sum_{k=1}^{pop\_size} eval(v_k) \tag{2.11}$$

where v_k is the kth chromosome in this generation, and, in the case of maximisation, $eval(v_k) = f(\mathbf{x})$. Next, the selection probability p_k must be determined, which is simply calculated by

$$p_k = \frac{eval(v_k)}{F} \tag{2.12}$$

The cumulative probability q_k is also needed, and can be found by:

$$q_k = \sum_{j=1}^{k} p_j \tag{2.13}$$

Next, to select which chromosomes are to be used to generate offspring, a random number $r_o \in [0,1]$ must be generated pop_size times. Then, for each chromosome, r_o must be evaluated in regards to q_k: If $r_o < q_1$, the chromosome v_1 is chosen, otherwise, the the kth chromosome larger than one is selected, if it fulfils $q_{k-1} < r_o \leq q_k$. This leads to the fact that if a chromosome scores high on the fitness function, it has a larger probability of being chosen for reproduction (and sometimes more than once), while it causes the chromosomes that scored low on the fitness function to be less likely to be chosen [29].

Step 5

This step handles crossover and mutation. A simple method to use for crossover, is the one-cut-point method, which takes two chromosomes, cuts them at a specified location, and swaps the bit string to the left of the first with the bit string to the left on the second, like shown below:

[1100011001]
[0100101010]
becomes
[1100 101010]
[0100 011001]

First, the chromosomes to be crossed is chosen. This is done by generating a random number $r_k \in [0,1]$, and choosing the kth chromosome as a parent for crossover if $r_k < p_c$, where p_c is the crossover rate. Next, the point of the cut is chosen by generating a random integer in the range from 1 to the length of the chromosome minus one (i.e., if the length of the chromosome is 33, the integer lies in the range $[1,32]$). Which chromosomes to be mutated are chosen much the same way as which chromosomes are to be crossed, however, the number of randomly generated number must be the number of genes in the population (i.e. the population multiplied by the length of each chromosome). That is to say, a list of numbers r_g must be generated, and must lie in the range $[0,1]$, while $g = 1,2,...,pop\_size \cdot chrom\_length$. The gene g is selected if $r_g < p_m$, and mutation is done by flipping that gene (i.e. flipping a 0 to 1, or a 1 to 0), illustrated below:

[1011 0 01011]
becomes
[1011 1 01011] [29].

Thus, a new population is created, and the steps 3 through 5 is repeated until a specified event occurs (which can be a predetermined number of generations, for instance). There are other aspects to GAs, and the methods discussed above may be substituted with more complex or more sophisticated methods, and there are specific algorithms to more complex or specific problems [29]. None of those will be discussed in this report; the algorithm presented above will suffice for the needs this project has.

The results of a GA can be graphically presented in an Evolutionary Progress Plot (EPP). This is a plot that depicts maximum, minimum, and average solutions of the fitness function as a function of generation [30]. All the chromosomes might be represented as dots in the plot along with the minima, maxima, and averages [31]. The

EPP may be a useful tool to evaluate the GA, as it shows how it converges across generations, and may be used to determine whether a reasonable number of generations has been chosen. Several runs through the GA might also prove useful, as it provides a better understanding of what an optimal solution might look like. Generally, it is unknown what such a solution looks like, and natural variation in the solutions are negated this way. It also gives insight into whether a right amount of generations are run or not [32].

2.8 Economy

2.8.1 Heat pumps

The *COP* factor is one of the key factors that play a role when evaluating the profitability of heat pumps, together with investments, and energy prices. To use a heat pump optimally, it is important that the temperature lift is relatively small (as the *COP* declines when ΔT is increased), which can be achieved by using the heat pump before peak load machines are connected, the temperature in the circuit should be as low as possible (without compromising its function), and to avoid couplings in the circuit that elevates the return temperature to a higher level than would have otherwise been the case [14].

Heat pumps generally have a large specific investment cost, but have a relatively low consumption of electricity compared to the heat they produce [14].

2.8.2 District heating

The price on district heating is stipulated in the Norwegian law *Lov om produksjon, omforming, overføring, omsetning, fordeling og bruk av energi m.m.* (Energiloven for short) [33], and is regulated by Norwegian Water Resources and Energy Directorate (NVE) [19]. Energiloven § 5-5 states that the price of district heating should not exceed the price of electric heating, and that the price should be derived from a fee for being connected to the heating grid, a fixed yearly fee, and from heat used [33]. Statkraft Varme AS divides the price on the heat used into three components for commercial clients; namely one component derived from the total heat used in the period, called Π_E, one component derived from the maximum power used in the period, named Π_P, and one component derived from the efficiency of the heat used in the period, denoted Π_{vol}. As of 01.01.2018, the period the power component is evaluated at was changed from the highest peak of the year, to the highest peak of the month. Π_{vol} takes into account the amount of water that circulates through the substations, as well as the temperature differences on the water in versus the water out. This component is subtracted from the price on energy used (which varies throughout the year), and then multiplied by the total amount of heat consumed in the period. The power component multiplies the maximum power used during the period, with the tariff on power [34, 35]. In total, the price is decided by:

$$\Pi = \Pi_E \cdot Q_{cons} + \dot{Q}_{max} \cdot \Pi_P \tag{2.14}$$

where Π indicates the price. Q_{cons} is the heat consumed, and $\dot{Q}_{max}$ is the maximum power delivered during the month. Π_P varies both with power consumed and by season. The tariffs are presented in tables 2 and 3. The term

Table 2: Power prices during summer and winter months, for commercial clients, during 2019. Data from [36].

$\dot{Q}$	Π_P [kr/kW/mo.]	
	Summer (March - October)	Winter (November - February)
0-200	45	60
200-500	40	53
500-800	35	47
>800	30	40

Table 3: Energy prices during summer and winter, for commercial clients, during 2019. Data from [36].

	Π_E [kr/kWh]
Summer	Elspot price+0.2648
Winter	Elspot price+0.2648 $-\Pi_{vol}$

0.2648 in table 3 is derived from different tariffs, while the elspot price is the monthly mean price determined by the Nord Pool Group. Π_{vol} is calculated by the following formula:

$$\Pi_{vol} = \frac{3600 \cdot 3.13}{\rho c_p \Delta T} \tag{2.15}$$

where 3600 is the number of seconds per hour, while 3.13 is a tariff on the volume, in [kr/m^3] [36]. The elspot price

indicates the current market price for electricity, which is controlled by the Nord Pool group. It is the official power exchange market in the Nordic countries, the Baltic countries, Great Britain, and Germany [37]. The price of the electricity is dependent on location and time; in addition, the demand and supply plays big role when it comes to deciding the elspot price [38].

2.8.3 Operational costs and economic life

An important factor to consider when evaluating the profitability of an investment is the annual operating costs. The operational costs can generally be divided into the following sections:

1. cost of capital, which includes cost of debt and depreciated costs,
2. operational costs, and
3. maintenance [14].

An accumulator tank's annual operating costs are assumed to be approximately 2% of its investment cost [39]. This figure is subtracted from the annual savings that may arise due to peak shaving [40].

Life expectancy of a component can be evaluated in two ways; namely technical and economic life expectancy. Technical life expectancy is for how long the component physically can operate, while the economic life expectancy is for how long it is economically feasible to use it, either due to high maintenance costs, or due to other technical solutions that may be developed and make the current technology obsolete [40]. The life expectancy of a TES tank ranges from 20 to over 40 years [41].

Residual value is another aspect that may affect the profitability of an investment. This is the expected value the component might have at the end of its life. If the component has a residual value, it is added as income at the end of its life [40].

2.8.4 Economic analysis

Money is generally worth more today than it is in the future. Thus, the Net Present Value (NPV) is introduced, which takes interest, risk, and yields on investments into account to calculate how much money in the future is worth today. Hence, it makes cash inflows and outflows comparable regardless of the time of the transaction. This can be used to evaluate whether an investment is profitable or not. The NPV is calculated via a discount rate, which takes into account the interest as well as the risk assessment [40]. The NPV can be calculated by:

$$NPV = \sum_{t=1}^{k} \frac{\Pi_t}{(1 + r_{NPV})^t} \tag{2.16}$$

where Π_t indicates a single time period of the net cash inflow-outflows, t indicates the number of time periods, and r_{NPV} indicates the return or discount rate that can be obtained from alternative investments [42]. k indicates the total number of years the investment lasts. Equation (2.16) can be used to derive equation (2.17):

$$NPV = \Pi_{diff} \frac{(1 + r_{NPV})^k - 1}{r_{NPV}(1 + r_{NPV})^k} \tag{2.17}$$

where Π_{diff} is the net cash inflow each year. This is a special case of the NPV method, and is generally called the Annuity Method of Depreciation, and it assumes the same cash inflow every year [40].

The deciding factor whether an investment is profitable will therefore be the NPV. If the value is positive, the investment will be advantageous as it is profitable, while investment with a negative value indicates a net loss and should be avoided [40]. One of the more significant disadvantages of this method is that it is dependent on assumptions about the future, as a project may often meet unforeseen events which requires additional investments to get started, or additional expenses may be needed after the project is finished. therefore it will be less accurate over a longer time period. However, the discount rate should take this somewhat into account [42].

The payback period (PP) is a simple method to evaluate how long it takes for an investment to become profitable. The method is appreciated for its simplicity, as it disregards the time value of money, and neglect the interest rate of the investment. Therefore it is widely used in practise, as it gives clear overview of the finance for the project. A drawback of this method is that the payback period does not take into consideration what happens after the payback, where it pays no attention to the overall profitability. It can be found by:

$$PP = \frac{\text{Costs of project/Investment}}{\text{Annual cash inflow}} \tag{2.18}$$

In the equation, PP represent the payback period, *investment* would be the costs that provided for the project to be set in motion, and *annual cash inflow* is the financial saving or income that is gained from the investment [40, 43].

3 Method

3.1 The local heating system

The local heating system which is to be assessed in this report is installed in NTNU's buildings NHL, Valgrinda 2000, Vassbygget, and Turbinlaboratoriet [44], but it will be referred to as only NHL in this report. The figure in appendix A is a depiction of the buildings that are connected to the same local heating system. The central heating system is designed as a 80/60 system, as explained in chapter 2.6.3. However, although the return and supply temperatures are designed at 80/60, the supply and return temperatures are rarely at these temperatures. The TES tank is meant for diurnal TES, and is located outside NHL. The system in question is connected to Statkraft Varme's district heating grid. The system consists of two heat pumps, one TES tank, several pumps, several heat exchangers, and a load – which is the energy consumption of the buildings – as well as instruments to measure, among other things, temperatures and mass flow rate. This, along with the heat exchangers connected to the district heating system, delivers heat to the central heating grid. A sketch of the system as it is evaluated in this paper is found in figure 8. The box in the top right corner of the sketch represents the load $\dot{Q}_{load}$.

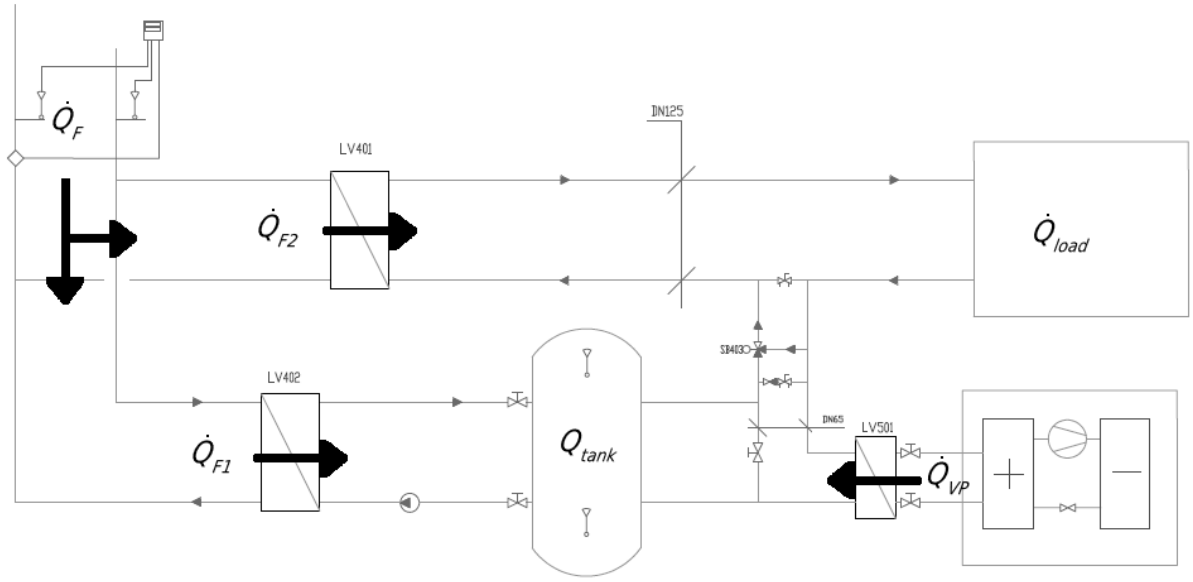

Figure 8: A sketch of the system evaluated in this paper. It is modified from the sketch in appendix B.

3.1.1 Heat exchangers

The system has three heat exchangers, as seen in figure 8. Two of the heat exchangers are directly separating the central and the district heating systems from each other, while another separates the heat pump from the central heating system. The total heat bought from Statkraft Varme AS is denoted as $\dot{Q}_F$ in figure 8, which consists of two parts: One directly to the load, called $\dot{Q}_{F2}$, and one that delivers heat to the tank, $\dot{Q}_{F1}$. This was done to more easily distinguish the amount of energy used to charge the tank in comparison to the total energy bought.

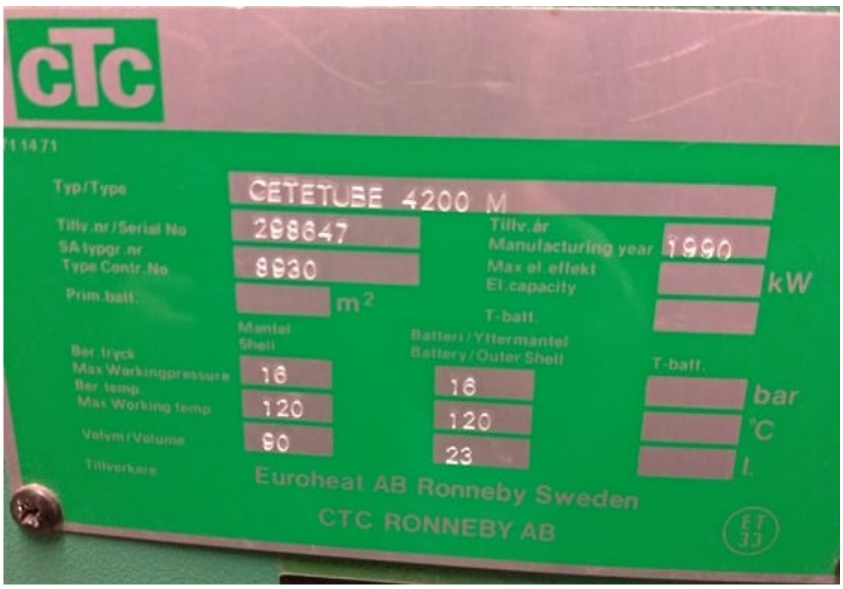

Figure 9: Nameplate of the heat exchangers at the NHL building.

NTNU did not have the data sheets for the heat exchangers [45], but the nameplate on the exchangers are presented in figure 9. The type Cetetube 4200 M was looked for online, where a datasheet from the company was found that seems to correspond with what was stated on the nameplate [46]. According to the datasheet, the maximum heat transfer rate through the heat exchanger is approximately 5MW. This seems to correspond with what is stated in chapter 3.1.3.

3.1.2 Heat pump

Only one of the heat pumps will be evaluated in this report, which is an air-to-water heat pump that utilises the outdoor air as the hot reservoir. The heat pump is connected to the local heating system, and is used to heat up the returning water for the local heating system. This allows the buildings to use more energy, where the temperature of the return water could be lower than what would otherwise be favourable, and the heat pump reheating the water before it flows through the heat exchangers connected to the district heating grid. This would be economically feasible due to the volume part of the district heating bill. There is also the possibility to use the heat pump for storing energy in the TES tank, as the local heating system has the ability to make a closed loop between the TES tank and the heat pump. The heat pump has some limitations when it comes to producing heat energy, where it can only heat the water up to 50°C. The heat pump that is utilised in the system is a SYSAQUA 140, and it uses the refrigerant R410A. The electric power input that is demanded from the heat pump for heating is 48.8kW, which gives an integrated full load efficiency (COP) of 2.15 [47]. The heat produced by the heat pump is denoted as $\dot{Q}_{VP}$ in figure 8.

3.1.3 Pump

The pump that is seen in figure 8 is used to circulate water through the tank. It is a MAGNA3 40-120 F, where the nominal volume flow rate is 12.6m^3/h [48]. This leads to it being able to circulate all the water in the tank in

approximately one hour. Verbal communications with staff engineer Olav Høyem also indicated that the pump was the limiting factor to how fast the tank could be charged and discharged. Thus, the turnover rate in the simulations will be set to one hour. The pump's performance will otherwise be omitted from the simulations.

According to the datasheet for the pump, it uses 427W to circulate water at full load [48]. This electric power is the main source of the tank's operating costs.

3.1.4 TES tank

The district heating system and the heat pump can charge the TES tank with energy and cover parts of the load that the NHL building demands. The energy stored in the tank at any moment is denoted as Q_{tank} in figure 8. On the other hand, when the TES tank discharges it will transfer energy by heating up the returning water in the local heating system.

The TES tank installed in the system is depicted in figure 10. The tank's dimensions are as follows:

- Inner diameter = 2494mm,
- outer diameter = 2703mm,
- total height = 3434mm,
- estimated inner height = 2456mm,
- volume = 12 000L, and
- maximum internal pressure = 3bar.

It is constructed in stainless steel [49], and it is isolated with two component polyurethane [50]. The tank will be evaluated at 1bar, and the maximum capacity of the tank was calculated with equation (2.6) to be 279kWh, where c_p was chosen to be 4.187kJ/(kg·K), and ρ was set at 1000kg/m^3. The internal volume mentioned in the list above is assumed to be the usable internal volume. The internal height of the tank is not provided in the datasheet, and it is unreadable in the schematic; it is therefore calculated to be 2456mm, based on the internal volume and the inner radius. The steel has a negligible impact on the heat losses as the thermal conductivity of steel, which is 17W/(m·K) [51], and is several orders of magnitude larger than for polyurethane. The insulation has a thermal conductivity of approximately 0.023W/(m·K) at around 315K [52]. 315K is used, as this is approximately the mean temperature of the insulation, by using the annual mean temperature in Trondheim (which is 5.6°C) [53], and the maximum temperature in the tank (which is 80°C). The heat transfer coefficient $h \in [5, 30]$ W/(m^2·K), depending on i.a. whether it is windy or not [54].

For the purposes of this report, the MB modelling approach will be applied to the tank, where the top volume is assumed to be 80°C, and the bottom section is assumed to be 60°C. This leads to the assumption that losses are only present in the top section of the tank. This model is chosen as it provides higher accuracy than the fully

mixed model, without compromising much simulation time, while also not being too complex. Convection on the inside will not be taken into account, nor any heat transfer between the two layers. The heat transfer coefficient $h = 20\text{W}/(\text{m}^2\cdot\text{K})$ is chosen, and $\Sigma R \cdot L$ of the tank walls are found by equation (2.5) to be 0.5628(m·K)/W. This figure is used in calculations in the model, and is multiplied by ΔT, which is calculated by taking the maximum temperature in the tank and the measurement of the outside temperature for that hour, and the height of the hot volume in the tank. The losses through the roof of the tank is also calculated, where equation (2.4) is used, where the geometry is assumed to be flat. The losses through the bottom area is neglected, as the temperature in the model is unable to drop below 60°C. If the tank is full, the air between the tank and the ground should be almost unaffected by wind, and should therefore insulate well, making the losses negligible in comparison to the walls and the roof.

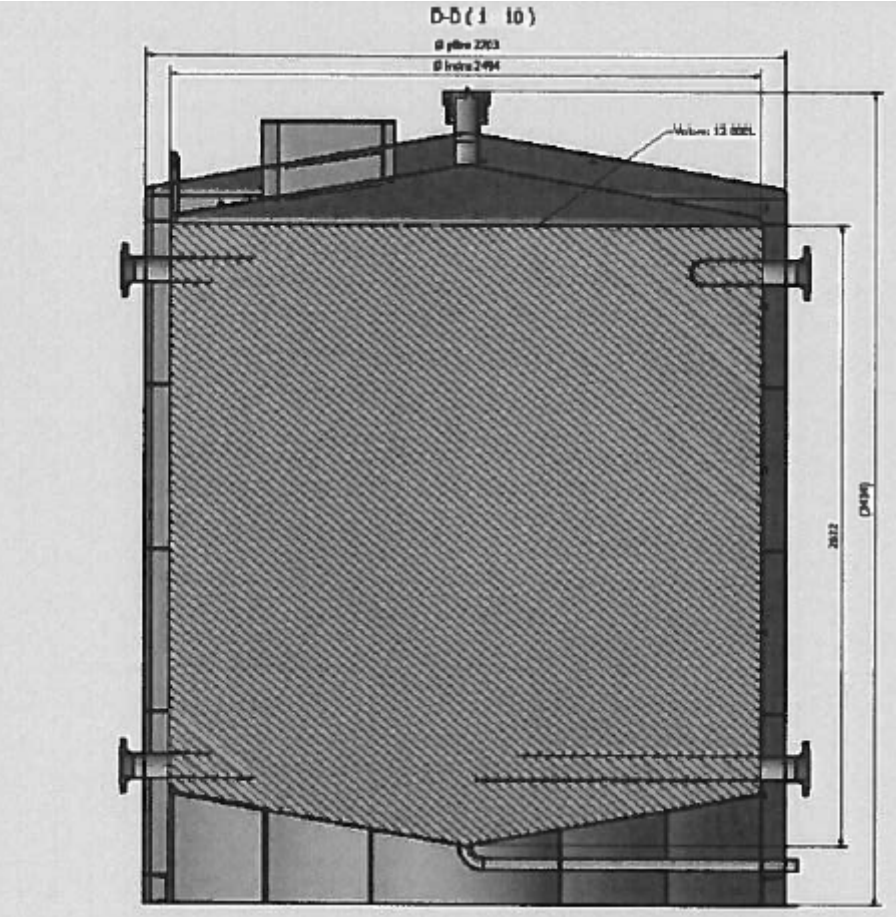

Figure 10: The TES tank from the data sheet [49].

3.1.5 Investment cost

Table 4 presents the total investment costs of the project at the NHL building, divided into different expenses. The investment cost for this project was covered by NTNU Campus Services Division, with a total cost of almost 1.1MNOK [55].

Table 4: Installation costs of the TES tank [55].

Description	Price [NOK], excl. tax
Cost of tank	436 000
Rig	10 000
Column drilling	15 000
Pipes and mounting	427 000
Upgrade of heat central	127 000
Electric work	44 953
Foundation	20 000
Total	1 079 953

3.1.6 Economic analysis

As stated in chapter 2.8.3, the annual operating costs of the tank is assumed to be 2% of the total investment cost from table 4.

In both case A and B, the *NPV* method presented in chapter 2.8.4 will be used to evaluate the profitability of the investments, through equation (2.16). As mentioned above, the life spans of the tanks evaluated are set at 20 years for case A, and the profitability is thus evaluated at this period. For case B, it is evaluated at both 20 and 40 years. 40 years is chosen because TES tanks can have an economic life for this long, as mentioned in chapter 2.8.3. Assistant professor and Vice Dean Audun Grøm suggested to use a discount rate at six or seven percent, to account for the actual interest rate, risk, and possible fluctuations in the price throughout the period. It was also stated that an investment like this is usually considered low risk [56]. Thus, 7% was chosen, as a larger percentage yields a more conservative result. The risk in the investment mainly consists of the tariffs on district heating which might change in the future. The heat pump and the tank might work in tandem in a way in order to reduce the need to buy heat from Statkraft Varme AS. This might assist in the reduction of the risk of the investment. One important factor that might have an impact in the future is the change of interest, which is one of the main reasons why the discount rate is set. If the interest rates increases, it might lead to the discount interest being too low. In spite of this, the rate of 7% should be suitable for this project. However, economic considerations are a secondary concern in this report.

7%, along with 20 years, is used in equation (2.17), the figure NPV/Π_{diff} was equal to 10.59401425. $NPV/\Pi_{diff} = 13.33170884$ when calculating it for 40 years. These figures will be respectively be multiplied by Π_{diff} to calculate the *NPV* in case A2 and B, and in case B. When calculating the *NPV*, the average savings of the two years are assumed to be the amount saved for every year of the economic life expectancy for the tank due to lack of data. According to Martin Sæterbø, the residual value of the tank is worth its weight in stainless steel, where the price is approx. 7.5NOK/kg, assuming that it wont be sold for further use. The tank's weight is calculated to be 1 500kg without insulation. The cost of removing the tank is also substantial, and is suggested to be between 7 000 - 13 000NOK, and accounts for both renting a crane and removing the tank [57]. Therefore, the residual value is assumed to be zero.

The *PP* of the project was calculated with equation (2.18) for both case A2 and B to get a more nuanced understanding of the investment.

3.2 Data inputs

The data used in the simulations are hourly measurements of the outdoor temperature, temperature on the inlet and the outlet water, and the volume flow rate, as well as the load. The load is, in the simulation, assumed to be equal to the heat bought from Statkraft Varme AS, i.e. excluding the heat produced by the heat pumps. This data was provided by NTNU. The electrical power delivered to the heat pump was also acquired, as well as datasheets for the different components. The monthly mean elspot price used in this paper are presented in figure 11.

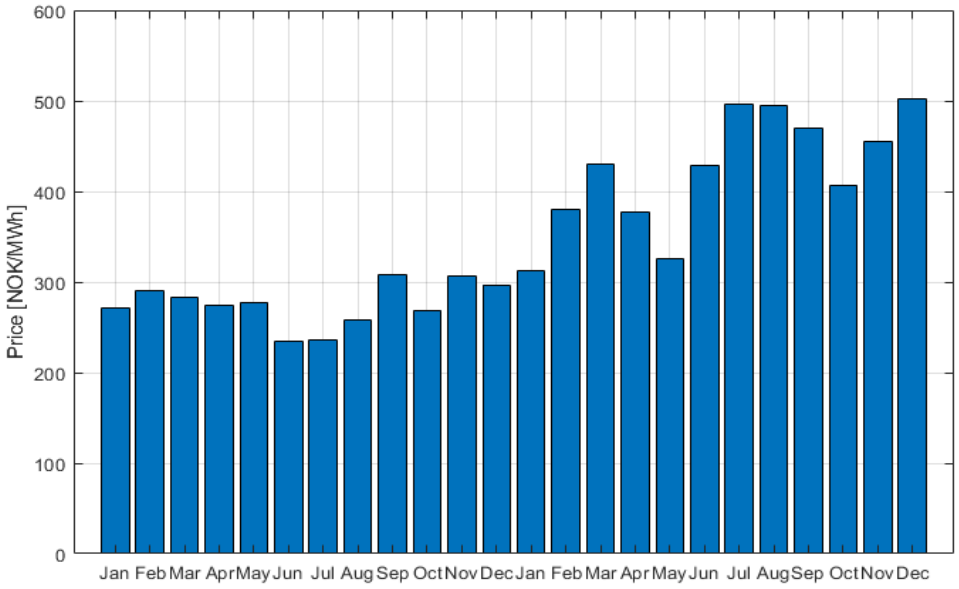

Figure 11: The monthly average elspot prices from 2017 and 2018, set by the Nord Pool Group. Data from [58, 59].

3.2.1 Data processing

The heat data provided by NTNU seemed to be calculated by the ΔT and mass flow rates, where ρ and c_p seemed to be at 1000kg/m^3 and 4.187kJ/(kg·K). This was confirmed when said values were used to calculate the heat with equation (2.6), and the difference between the provided and calculated values seemed to stem from rounding differences. Other data from NTNU contained electric power used by the buildings in question over the same period. The raw data contained measurement errors that needed to be corrected before calculations could be conducted. This resulted in an adjustment of extreme ΔT values, and missing outdoor temperatures were inserted.

The missing outdoor temperatures were replaced with zero, as a majority of the values were changing from positive to negative in-between the missing values, and the remainder being close to zero. Thus, this way seemed like the most efficient, and most realistic, course of action.

The extreme ΔT measurements were present in the raw data due to the fact that little to no heat had been used in the hours prior, causing the measurements to be inaccurate. Staff Engineer at Campus Services Section Øystein Engan proposed to eliminate all measurements above 80°C [60]. This was confirmed with a histogram plot of the measured values, as shown in figure 12.

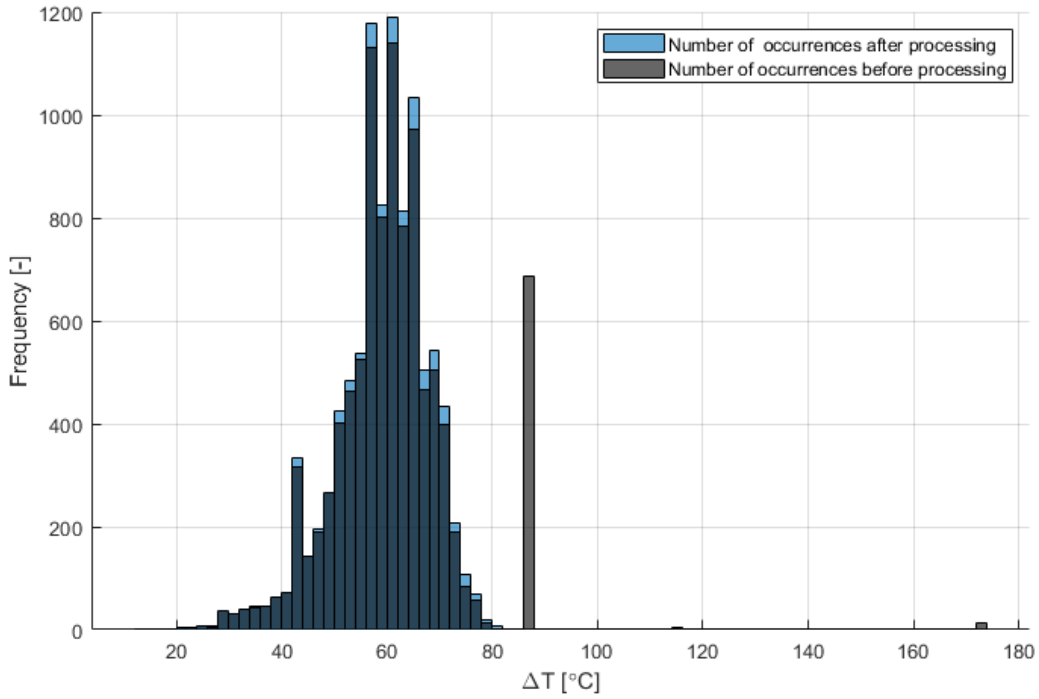

Figure 12: Histogram depicting measurements of ΔT before and after the data were processed.

Figure 12 depicts the measurements before and after the processing, where values that are zero in the data set are omitted, so as to better identify outliers. However, they are included in the data set when calculations are executed. The black bars represent the measurements before processing was conducted, while the blue bars after the processing. It appears from the shape of the histogram that the values above $\sim$80°C stands out, and seems to be deviating from the bulk of the data in a significant way. Furthermore, the temperature data both the hour before and after the peaks were comparatively lower, and a simple linear interpolation was used to average out the peaks above 82°C. The difference in power was calculated by equation (2.7) to be $\sim 5.3 \cdot 10^4$kWh, or two orders of magnitude less than the total heat consumed over the two year period before the temperatures were processed, and it was deemed adequately close enough to be used in further calculations.

One hour was missing from the data from NTNU, namely the hour skipped because of daylight saving time in March 2018. This change did not occur neither in March 2017 nor October for any of the two years. To correct for this, one hour was added in March 2018, where the power demand and the remaining values are equal to the average of the hour before and after.

3.2.2 Data: patterns and analysis

Figure 13 shows how the load of the building changes with the outside temperature, based on the data from NTNU. The orange circles within the diagram represent the average energy consumed at each temperature interval of 1°C. The graph seems to have a semi-linear tendency from -20 °C to 10°C, where it breaks and flattens out. After $\sim$25°C, the heat consumed by the building goes to zero. The shape can be explained by the fact that after a certain outdoor

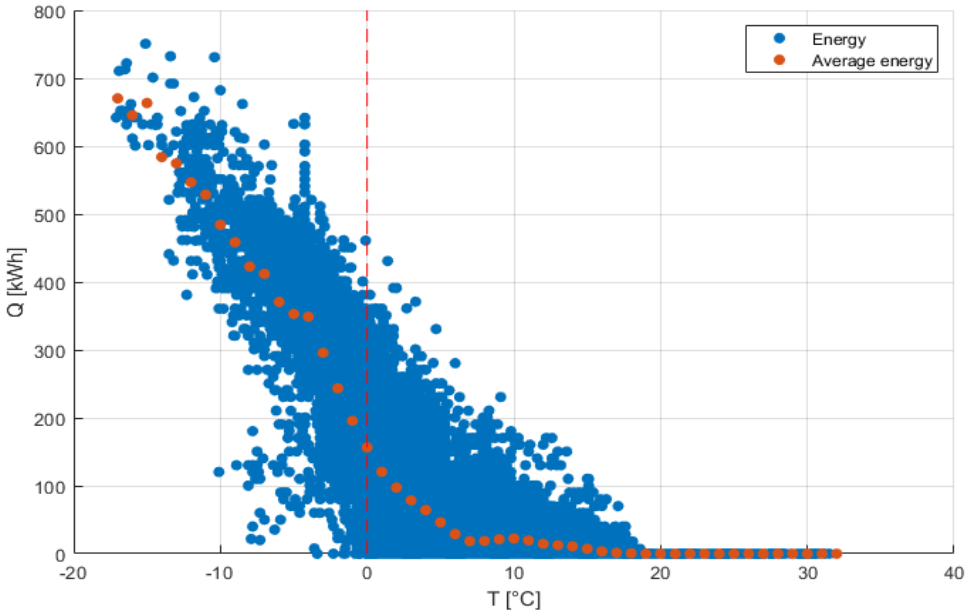

Figure 13: ET diagram showing how the load of the building changes with the outside temperature.

temperature, there is no more need to either buy or produce heat, as conduction from the outside is enough to meet the load (or maybe even ventilation is needed to reach comfortable indoor temperatures). Ideally, as mentioned in chapter 2.6.2, the energy usage should align itself linearly as the temperature increased, and there should not be much spread along this linearity. However, this is not the case. This might be explained by the fact that not all the energy in the building is accounted for, as none of the heat pumps' heat production is included in the plot. Another possible cause for the non-linearity and the large spread in the usage arises when the use pattern of the building is considered. One of the buildings connected to the central heating grid contains a hydropower laboratory, where the heat usage is probably dependent on the its activity pattern. If the laboratory is used sporadically, the heat usage may reflect this. Lastly, it might reflect a non-optimal control strategy for when the valves to the district heating network open and close, and how much they open when they do.

Figure 14 shows how the average heat demand of the building changes daily for both seasons. Both curves have some shared features, where they start the day with a comparably low value, then they increase until they reach a peak at around 05:00 during the summer and 09:00 during the winter, where they have a relatively high load until midday. Then they decrease until a minimum value is reached at around 15:00, and then starts to increase slowly back to the starting value. This pattern is caused by the HVAC system. It is demand-controlled, resulting it being reduced during the weekends and holidays as to save money and to work towards the environmental goals. As the data used in the simulations were historical data, the activity in the building and the HVAC system are accounted for indirectly.

The factors discussed above causes that there are, on an average day, a surplus of heat present during the afternoon and during nighttime; these periods create suitable conditions for charging the TES tank.

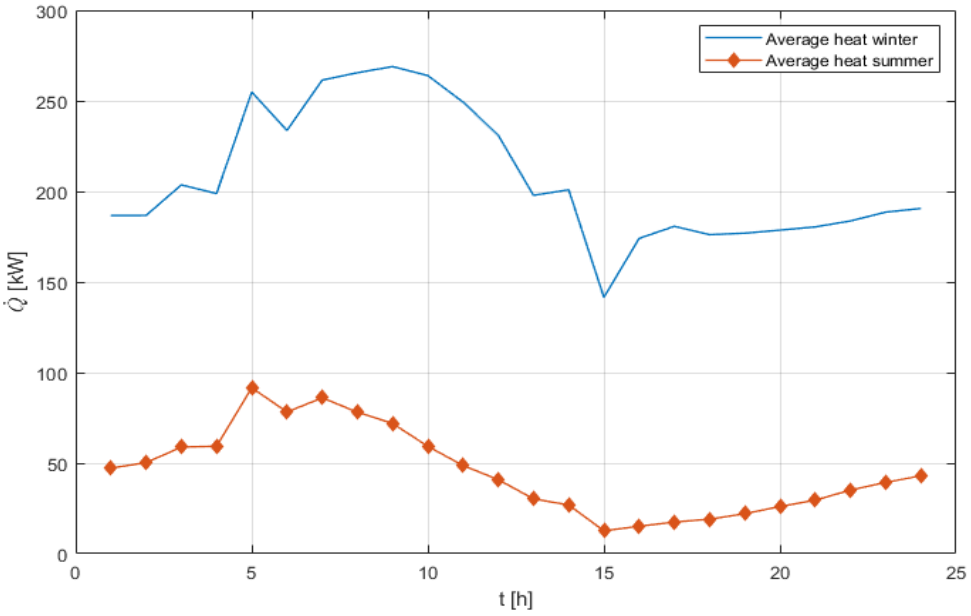

Figure 14: Average load of the building for a day during winter (blue) and summer (red).

3.3 Case A

Case A is separated into two different stages, A1 and A2, where A1 tries to optimise the use of the TES tank on a daily and weekly basis, keeping in mind how much to shave the power peaks over the period. The results of this scenario were then run in a GA in case A2, where it tries to optimise the problem with regards to the difference in price before and after the tank was installed in the system.

3.3.1 Case A1

To achieve an optimal use of the TES tank, a realistic time period was chosen, which was either daily or weekly consumption of district heating. This is chosen due to the inaccuracy of weather forecasts over longer periods of time. The heating needs are dependent on the outdoor temperatures to a certain extent. Therefore, having a reliable weather forecast is crucial to plan for the potential upcoming power peaks. However, as this model uses historical data, it is also possible to extend the periods to months.

A target line $\dot{Q}_S$ is introduced to determine at which level the peaks should be shaved. This is done to utilise the energy stored in the tank optimally, where the load above the target line should be covered by the tank, and the energy in-between the load and the target line is used to charge the tank. The target value is constant for a given time period. If there are a mix of peaks with a lower load in-between, the tank will also charge. The goal is ultimately to shave the peaks so as to have a load that is as equal to $\dot{Q}_S$ as possible, and also to utilise as much of the available heat as possible.

The model is written in MATLAB, and the script may be viewed in appendix C, and the prices are calculated in the MATLAB script in appendix D. MATLAB was chosen due to its availability through the NTNU license, as well as it being part of a subject TFNE1002 at NTNU.

The method used to find an optimal $\dot{Q}_S$, starts of by finding the average value of the load for the specified period. After $\dot{Q}_S$ is set, the script starts a for loop that simulates the system hour by hour. It calculates the heat stored in the TES unit and the load. This simulation is packed inside a while loop, which is not ended until the results are sufficient. When the ending requirements are met, it starts to simulate the next period, starting by finding a new $\dot{Q}_S$ for that period. The optimisation and its constraints can be formulated as:

$$
\begin{array}{ll}
\text{Minimise} & \dot{Q}_{S,i} \\
\text{subject to} & \Delta\sum_{j=1}^{m}(Q_{tank,j}) \in \left[\sum_{j=1}^{m}(\dot{Q}_{load,j}-\dot{Q}_{S,i})-0.001, \sum_{j=1}^{m}(\dot{Q}_{load,j}-\dot{Q}_{S,i})\right\rangle \\
\text{and} & \dot{Q}_{S,i} \geq \dot{Q}_{F,j} \\
\text{and} & 0 \leq Q_{tank,j} \leq Q_{tank,max} \\
\text{and} & \begin{cases} \min\{Q_{tank}\} < 0.001, & \text{if } \sum_{j=1}^{m}(\dot{Q}_{load,j}) \geq Q_{tank,max} \\ \min\{Q_{tank}\} \leq Q_{tank,max} \end{cases}
\end{array}
$$

In this case, $i = 1,2,...,n$, and $j = 1,2,...,m$, where n is the number of periods in the simulation (i.e. the number of days or weeks), while m is the number of hours in said period. $\Delta\sum_{j=1}^{m}(Q_{tank,j})$ represents the change of the energy in the tank; this includes the state of charge in the beginning and the end, as well as the losses and the delivered heat. The reason why 0.001 is included, is to get a margin of error to reduce the computation time, while still maintaining the accuracy of the model. The last constraint is only true when the system is simulated for weeks.

If these conditions are not met, $\dot{Q}_S$ changes accordingly. For example, if the TES tank is not utilised enough, $\dot{Q}_S$ will decrease in value. This is done by multiplying the current target value with 0.98. On the contrary, if the heat stored is insufficient, the line will increase in value by multiplying with 1.01, to attempt to find a new value which meets the conditions. This procedure will continue until the conditions presented above are met.

One important output of the program is the difference in price before and after. Equations (2.14) and (2.15) are used to calculate the price before and after, and $\Pi_{diff} = \Delta\Pi$. The script calculates the costs of the two years with and without the tank included in the system. The energy, power and total price for both alternatives are also calculated.

A balance was introduced in the script to make sure the energy in and out is equal, and to make sure that the model acts according to the first law of thermodynamics. The balance is defined as

$$Q_{balance} = \sum_{i=1}^{m}(\dot{Q}_{F,i} - \dot{Q}_{load,i} - \dot{Q}_{loss,i}) + Q_{tank}(1) - Q_{tank}(m) \tag{3.1}$$

That is, it sums the energy in and energy out, and it should be equal to zero.

The calculations in the simulations are conducted at the end of each hour because the data inputs were sampled at every hour.

Finally, the efficiency of the tank was calculated, for both the weekly and daily consideration. Equation (2.8) was used to calculate the efficiency, and with the parameters used in this report, it looks like:

$$\eta = \frac{\sum_{i=1}^{m}(\dot{Q}_{load,i} - \dot{Q}_{F2,i}) + Q_{tank}(m)}{\sum_{i=1}^{m}\dot{Q}_{F1,i} + Q_{tank}(1)} \tag{3.2}$$

This efficiency was calculated over the whole two-year period.

3.3.2 Case A2

In this case, the output $\dot{Q}_S$ from case A1 were used as inputs to a GA, so as to try to optimise the simulation with regards to the price difference Π_{diff} before and after the tank was installed. It can be formulated as:

$$\begin{array}{lll} \text{Maximise} & \Pi_{diff}(\mathbf{x}) & \\ \text{subject to} & \Pi_{diff}(\mathbf{x}) \geq 0 & \\ \text{and} & 0 \leq x_i < 750 & \text{where } i = 1,2,...,n \end{array}$$

$\mathbf{x}$=$[x_1, x_2, ..., x_n]^{\mathrm{T}}$, and n is the number of weeks or days in a year, depending on whether inputs are evaluated on a daily or weekly basis. $\mathbf{x}$ in this case represents the vector derived from $\dot{Q}_S$. The script containing the GA was written from scratch, and can be found in appendix E.

The formula described by Gen & Cheng, described in chapter 2.7.1, were utilised to make the algorithm. The bit string representation was used, but instead of having one large string, it consists of an $n \times 1$ cell, where each row in the cell is a 64-bit binary string. n is the number of days or weeks in the year, depending on whether daily or weekly considerations are made. The initial population were generated by multiplying $\dot{Q}_S$ with a randomly generated number in the range $[0.7, 1.3]$, and the inputs were encoded to binary strings with the tool written by Verner [61]. The original input were kept, in case this was already the optimal solution. The script used in case A1 were adapted to be compatible with the GA, and were used as the objective function, while the difference in price were used as the fitness function. Equations (2.11) through (2.13) were used to calculate the total fitness, the selection probability, and the cumulative probability at each generation. All the randomly generated numbers were generated with MATLAB's integrated random number generator.

The GA was executed twice; once for daily inputs, and once for weekly inputs. For both simulations, a population size of 20 were chosen, and the crossover rate and mutation rate were set to $p_c = 0.35$ and $p_m = 0.01$ respectively. These rates were chosen to create more variation within a generation and to explore more of the feasible region, while also not creating too much noise, and not to have unnecessarily long computation times. were set to three, which caused the $\dot{Q}_S$ to have the accuracy of 1W. The GA was run for 200 generations for both the daily and weekly considerations. The reason why 200 generations and 20 chromosomes were chosen, was, after initial testing of the GA, the changes were found to be negligible.

3.4 Case B

To get a rough overview whether the TES tank is of a optimal size or not, and possibly to find the best size, case B is introduced.

To be able to compare the tanks of different sizes, the installation costs of the different tanks are assumed to be equal. This excludes the investment cost of the tanks itself. This leads to the only variables to change to be the volume, radius, and price of the tanks, where the radii were calculated by the volume and height. The prices are estimates given by Martin Sæterbø at Skala Fabrikk AS [50], and are presented in table 5.

The simulations will be completed in the same order as in case A, with the same model, by first running the deterministic optimisation. The output of these simulations will be used as input for the GA to enhance the results further. Furthermore, the *NPV* values of the different investments will be calculated. And lastly, as with case A, the efficiencies of the tanks will be calculated.

Table 5: The different sizes of the tanks, as well as the prices and radii provided by Skala Fabrikk AS [50].

Volume [m^3]	Price [NOK]	Radius [m]
7	410 000	0.806
10	420 000	0.963
14	435 000	1.140
17	470 000	1.260
22	490 000	1.430

As mentioned earlier, table 5 shows the prices and geometries of a selection of tanks. According to Martin Sæterbø, the main reason why the prices differ is that the amount of material used will change. However, the utilisation of the material is a more important factor, therefore the prices changes marginally. The working hours required to create a larger tank does not change significantly either. However, if the tanks height were increased, another plate had to be added [50], which is assumed to have a greater impact on the prices. This leads to the assumption that the height is kept equal for all the tanks, and the radii are calculated thereafter.

Because the same script was used in case A and B, and the tank was able to charge and discharge completely in case A, which caused it to behave the same in case B. However, as mentioned in chapter 3.1.3, the pump can only deliver 12.6m^3/h at maximum capacity, causing all the tanks above 12m^3 to be unable to fill within an hour. This was tested to see if it had an impact on the simulation, where the test indicated that it did not; this occurred exactly once for each of the tank sizes above 14m^3 during the two years. As mentioned in chapter 2.3.4, the economic analysis

yields inaccurate results when determining the optimal storage size. However, due to the simplicity of the model, the performance of the tank will be determined by reductions in price and the first-law efficiency, where only the heat losses will be accounted for – it is assumed that the effectiveness of the tank is equal to one, and the second-law efficiency of the tank will not be evaluated.

4 Results

4.1 Case A

The results in this chapter will be separated into A1, A2, and peak shaving. A1 exhibits the results from the deterministic optimisation approach, while results for A2 presents the results from the GA optimisation. The tables and figures try to summarise the results from the simulations, which will be discussed in the next chapter. All the figures are based on the results from the GA.

4.1.1 Case A1

Table 6: Table showing the economical aspects of the simulations before and after the tank is included on a daily and weekly basis when forcing the tank to discharge completely.

	Before [NOK]	Daily after [NOK]	Weekly after [NOK]
Power	451 937	347 813	346 114
Energy	998 385	1 002 023	1 002 360
Total	1 450 322	1 3498 368	1 348 474
Saving	-	100 485	101 848

Table 6 presents the economical aspects of the simulations for the deterministic optimisation approach, for the daily and weekly periods. The daily values did not require the tank to discharge completely, unlike the weekly. Weekly had in total better results than daily, with a difference of $\sim$1 400NOK. It appears that the energy price is almost equal in the different considerations, while the power price contributes to the difference in savings.

4.1.2 Case A2

The results of the optimisation with the GA is summarised in table 7. It shows the best generation and the best chromosome within that generation, as well as the maximum price difference, on both a daily and a weekly basis. The difference in the required generations for the maximum values varied significantly, between daily considerations finding the optimum towards the end, while weekly found it in the beginning. The maximum value for the weekly is $\sim$102 100NOK, which is $\sim$1 400NOK higher than for daily.

Table 7: The generation and chromosome, as well as the fitness score, from the GA.

Daily/weekly	Generation	Best chromosome	Maximum price difference [NOK]
Daily	192	16	$\sim$100 700
Weekly	11	15	$\sim$102 100

In figure 15 and 16, one can see how the GA approach processes the data and finds the optimal result. For each generation the maximum and median are plotted, while all the chromosomes are represented as black dots

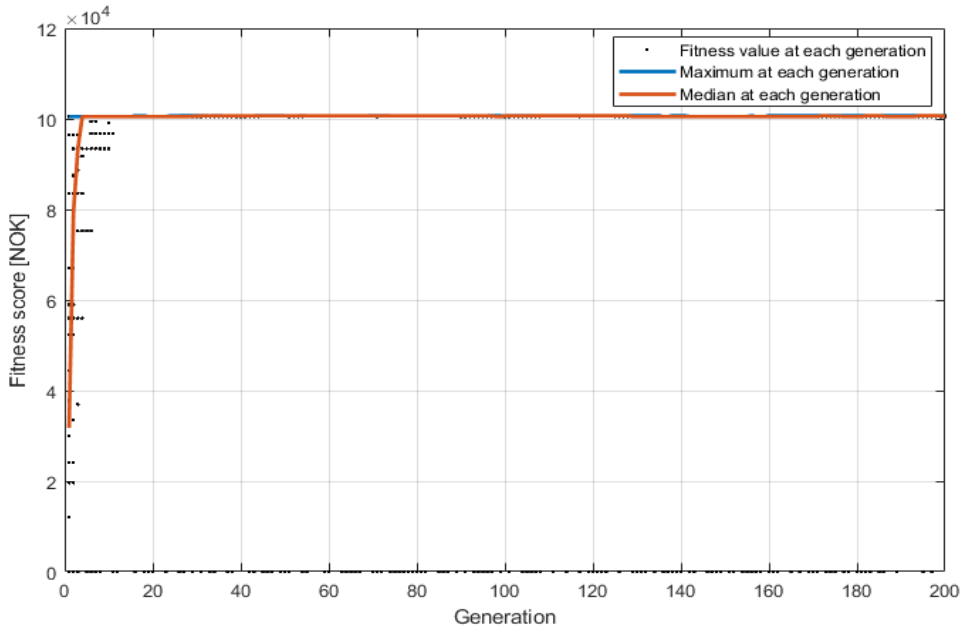

Figure 15: Evolutionary progress plot for the GA, for the daily consideration.

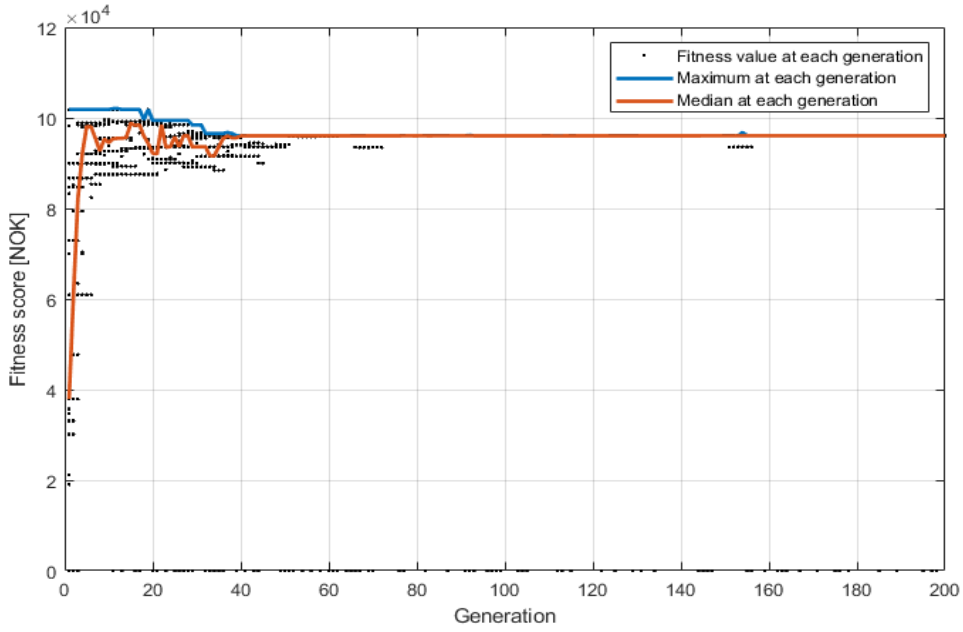

Figure 16: Evolutionary progress plot for the GA, for the weekly consideration.

in the plots. They seem to converge relatively quickly, where the maximum and median at each generation coincides. The maximum of figure 16 seems to deviate from the maximum at previous generation around generation 20.

Table 8 summarises the energy and power price, as well as the price difference, with the use of the GA approach, for both weekly and daily values. As in table 6, the power price is the main contributor to the price difference before and after the tank simulations.

Table 8: Prices divided into power and energy, with $\dot{Q}_S$ set to the output from the GA.

	Before [NOK]	Daily after [NOK]	Weekly after [NOK]
Power	451 937	347 813	346 114
Energy	998 385	1 001 805	1 002 146
Total	1 450 322	1 349 618	1 348 260
Savings	-	100 704	102 062

4.1.3 Peak shaving

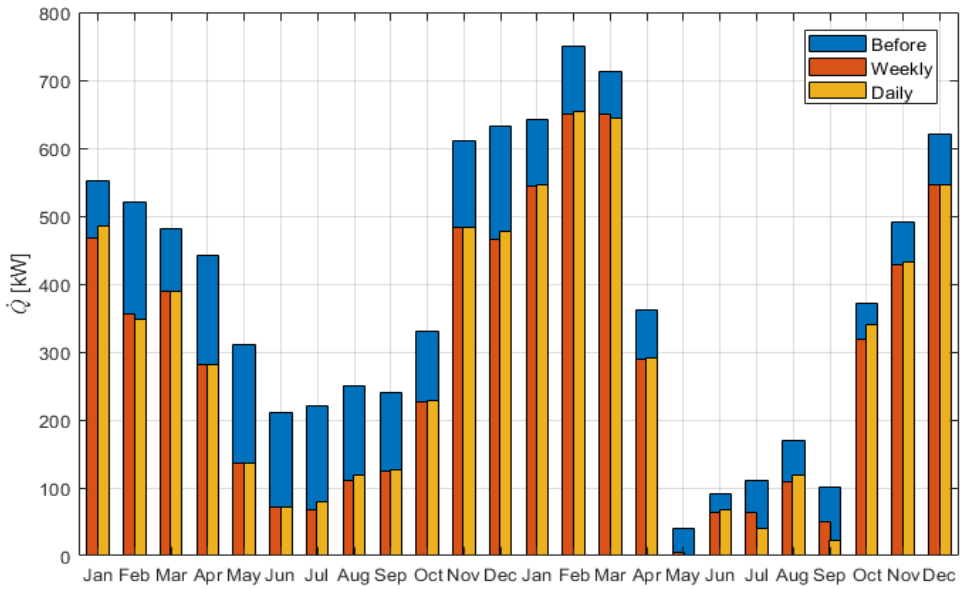

Figure 17: The maximum peaks before and after the TES tank is included in the simulations with daily and weekly values.

Figure 17 shows the daily and weekly reduction of max loads for each month after the simulations are conducted. The daily consideration cuts more at February 2017, March, May, July and September 2018. In the remaining months, they are either equal or the weekly consideration have larger reductions. An interesting observation is that the maximum peak in February and March 2018 are equal for the weekly consideration after the simulations are conducted. June and July 2017 and 2018 appears to be cut to the same level for the weekly consideration, however, they are not. The reduction in power peaks are generally cut more in 2017 than in 2018. The power peaks are also generally larger in 2017 than in 2018, with the exception of January through March.

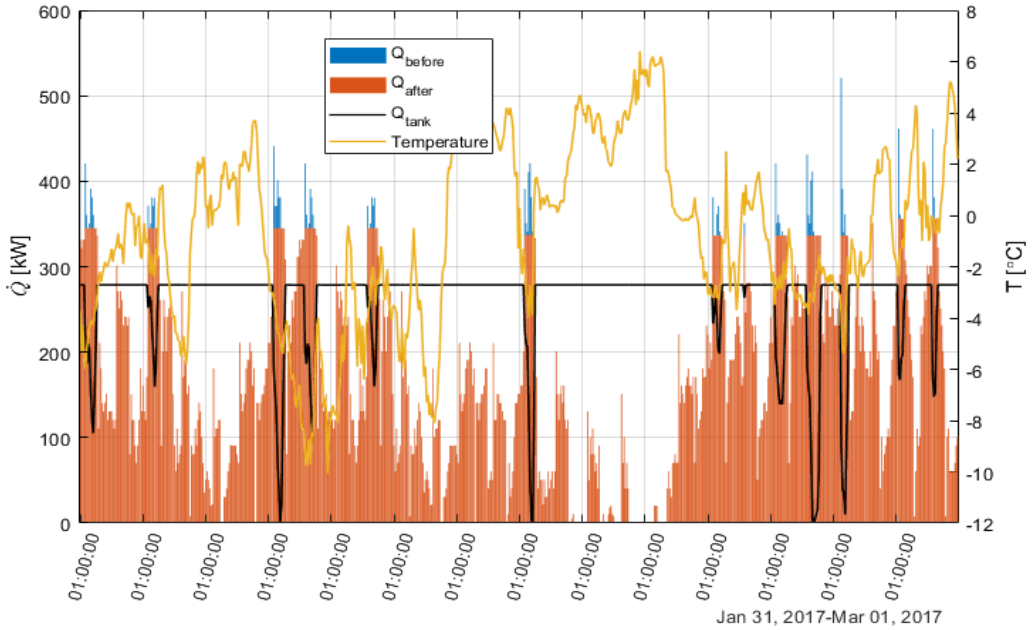

Figure 18: The results from the simulations for weekly district heat consumption in February 2017. The figure includes the heat requirement before and after the tank is installed, as well as the energy stored in the tank and the outdoor temperature.

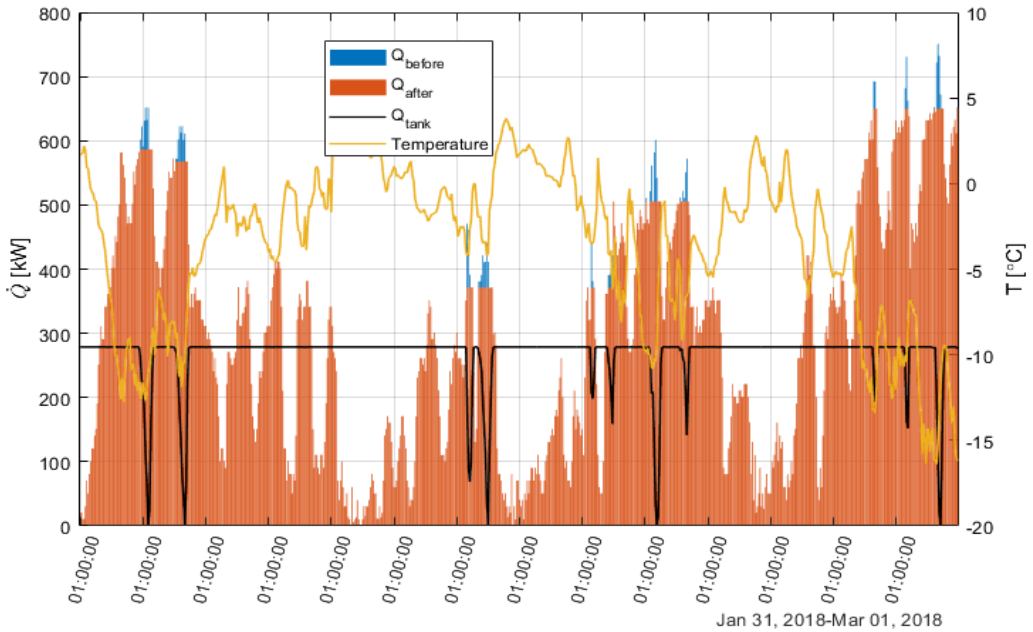

Figure 19: The results from the simulations for weekly district heat consumption in February 2018. The figure includes the heat requirement before and after the tank is installed, as well as the energy stored in the tank and the outdoor temperature.

Figures 18 and 19 show the simulations for district heat consumption for February 2017 and 2018. During February 2017, the temperatures and district heat consumption fluctuated considerably, while in 2018 they were more stable over longer periods of time. The peaks in 2017 were quite even, with only one extreme value at ∼520kW, and often had well-defined daily peaks. In 2018 the peaks were broader, and lasted for a several days at a time and was generally higher than the year prior. It is also apparent that it was generally colder in February 2018 than in 2017.

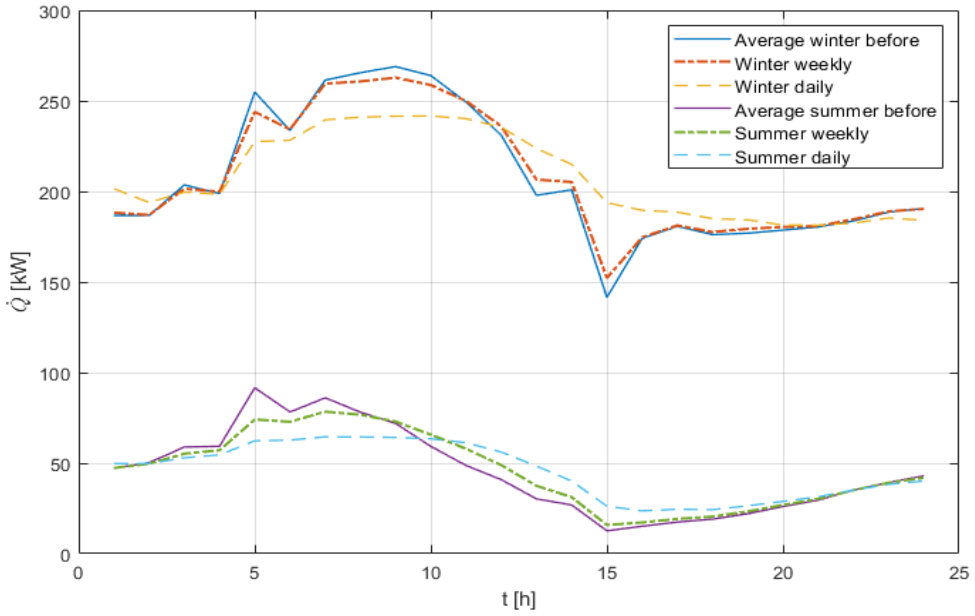

Figure 20: The average load shift for weekly and daily considerations, as well as the average load before the simulations, for both summer and winter months.

Figure 20 presents the average loads every hour throughout the two years, over the period of 24 hours. It is divided into summer and winter, and the average load shifts for both the daily and weekly consideration are present. The values before the simulation have the highest peaks regardless of the season. The weekly values are shifted slightly, where the maximum is lower, and the minimum is higher. The daily values displays a more significant load shift. The loads, independent of it being summer or winter, have the same general shape, with a maximum at around 05:00, and a minimum at around 15:00. Figure 21 shows the differences between the energy demand of the building

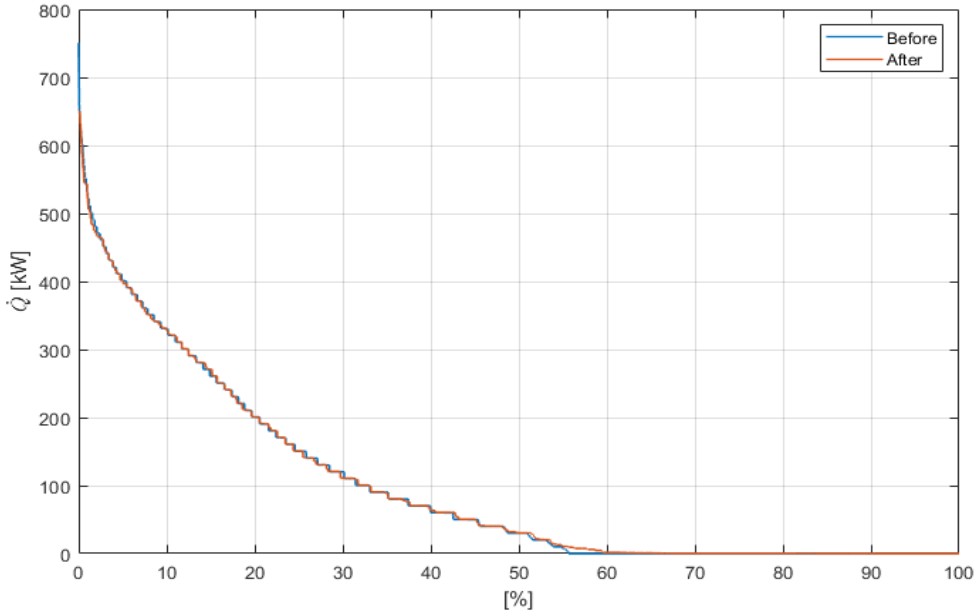

Figure 21: The duration plot shows the energy consumption before and after the simulations with the TES tank added to the system, for the weekly considerations.

before and after the TES tank was added for the weekly considerations. The peaks in the figure is located at around 650kW, in comparison to prior values, where the highest peak was at 750kW. In general, the duration curve after is lower than the duration curve before at the left side of the diagram, while on the right, the opposite is true.

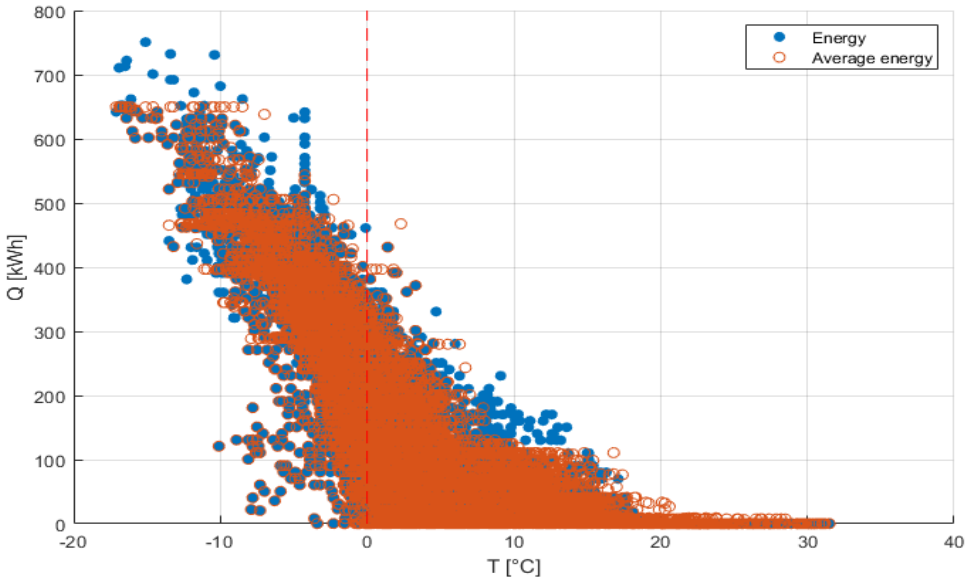

Figure 22: The ET diagram shows how the loads are shifted for weekly values.

Figure 22 presents the ET diagram for the simulations before and after the TES tank is included in the system for the weekly consideration. It appears from the figure that the load is broader before compared to after the simulations are executed. The district heating is hardly used after the outdoor temperature reaches 18°C. The most extreme values of the load is capped at around 650kW down from around 750kW.

The efficiencies were calculated to be 0.963 (96.3%) and 0.888 (88.8%) for respectively the daily and weekly considerations.

4.1.4 Economic analysis

Equation (2.17) was used to calculate the *NPV* for the economical analysis. The results are summarised in table 9.

Table 9: The *NPV* calculated from the results of the simulations, for both daily and weekly considerations.

	Daily	Weekly
Investment cost [NOK]	-1 079 953	-1 079 953
Average yearly savings [NOK/year]	50 352	51 031
Operational costs [NOK/year]	-21 599	-21 599
Net cash inflow [NOK/year]	28 752	29 431
NPV [NOK]	-775 344	-768 151

The *NPV* of the investment was calculated to be -768kNOK for weekly considerations and -775kNOK for daily.

The payback periods for the project was calculated with equation (2.18) to be 38 years, and 37 years, for the daily and weekly consideration respectively.

4.2 Case B

4.2.1 Tank performances

The efficiencies of the tanks are summarised in figure 23. The figure illustrates that the daily consideration has a steady efficiency with almost no visible change in efficiency with the increasing tank size, except from 7 to 10m^3. The weekly consideration, however, changes more profoundly with increasing tank volumes. The efficiencies from the weekly consideration are produced by the GA optimisation approach, while the efficiencies from the daily consideration are produced by the deterministic optimisation approach.

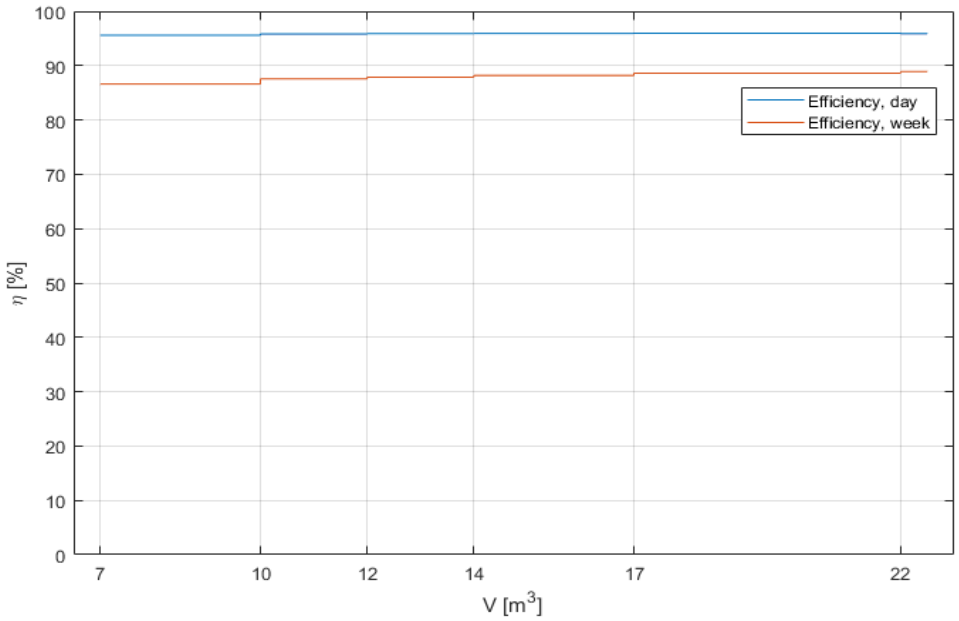

Figure 23: Efficiencies of the tanks, for weekly and daily values

All the power cuts from the weekly consideration can be seen in figure 24. In general, the largest tanks reduce the peaks more than the smaller. Two notable exceptions are July and September 2018. In July 2018, the smallest tank performs second best, while the best is the largest. In September, all the peaks are shaved to the same level.

4.2.2 Economic aspects

Table 10: Prices from the deterministic optimisation method for different sizes of the TES tanks, for daily and weekly considerations.

Volume [m^3]	Daily after [NOK]	Weekly after [NOK]
7	83 825	83 757
10	94 088	95 084
14	103 860	106 666
17	108 249	112 459
22	113 605	121 260

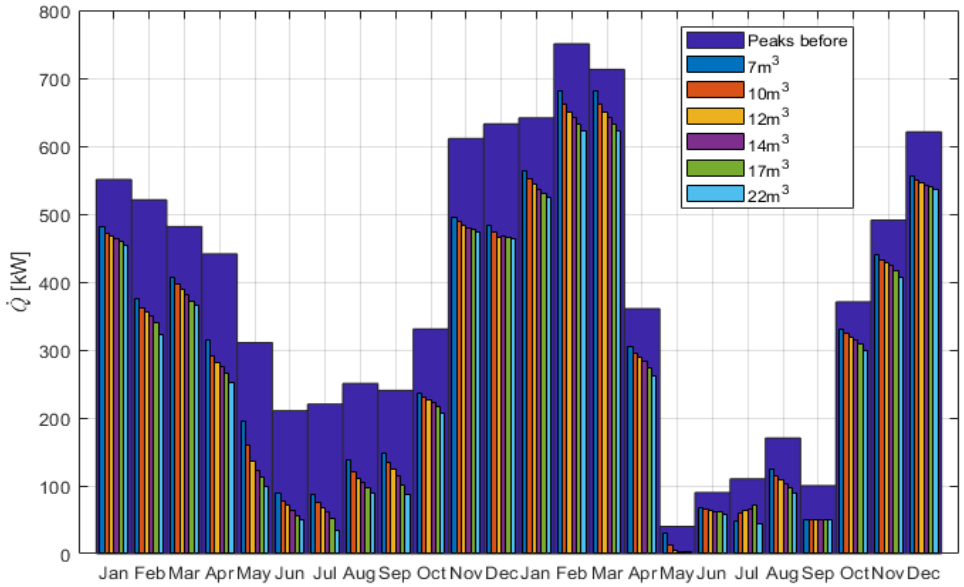

Figure 24: Power cuts from the different tanks, for the weekly consideration.

Table 10 presents the savings over a two year period with the different sizes for the TES tanks, with a total saving of 121 260NOK with a 22m^3 tank for the weekly simulation. There was a total difference of ∼8 000NOK between daily and weekly considerations for the aforementioned tank. All the price differences was acquired with the deterministic optimisation strategy.

Table 11: The results from the economic analysis of the different sizes for the tank, showing the investment costs, average savings, expenses, cash inflow per year and the *NPV*, assuming a life expectancy of 20 years.

Volume [m^3]	7	10	14	17	22
Investment cost [NOK]	-1 069 953	-1 069 953	-1 094 953	-1 129 953	-1 149 953
Average yearly savings [NOK/year]	41 960	47 542	53 513	56 380	60 632
Operational costs [NOK/year]	-21 399	-21 399	-21 899	-22 599	-22 999
Net cash inflow [NOK/year]	20 560	26 143	31 614	33 781	37 633
NPV [NOK]	-852 135	-792 994	-760 032	-772 080	-751 270

Table 11 presents the results of the economic analysis of case B. The results are all from the weekly consideration. The GA optimisation approach was utilised to produce the average yearly savings. The table indicates that the investment with the least losses is the tank with internal volume of 22m^3, where the *NPV* is approximately -751kNOK. The tank with the greatest economical losses would be the one which contains 7m^3, which has a loss of approx. -852kNOK. The tank with internal volume of 17m^3 is noticeably less profitable than both 14m^3 and 22m^3. The difference in *NPV* for the best and the second best tank is ∼9 000NOK.

The payback periods for the different tank volumes are presented in table 12, where the amount of years and months it takes before the investment is profitable are listed. The tank with a volume of 22m^3 is the one with the shortest

Table 12: Payback periods for the different tank volumes.

Volume [m^3]	*PP* [Years]
7	52
10	41
14	35
17	34
22	31

payback period, which is 31 years. The tank that has the highest payback period is the one of $7m^3$, which takes 52 years before is profitable. Table 13 presents the resulting *NPV*s if the the *PP* is considered, and the economic life expectancy is set at 40 years – which is approx. the average *PP* of the tanks – instead of 20.

Table 13: The *NPV* of the simulations with the GA optimisation approach, where the life expectancy is set at 40 years.

Volume [m^3]	7	10	14	17	22
Investment cost [NOK]	-1 069 953	-1 069 953	-1 094 953	-1 129 953	-1 149 953
Average yearly savings [NOK/year]	-21 399	-21 399	-21 899	-22 599	-22 999
Operational costs [NOK/year]	41 960	47 542	53 513	56 380	60 632
Net cash inflow [NOK/year]	20 561	26 143	31 614	33 781	37 633
NPV [NOK]	-795 847	-721 423	-673 482	-679 599	-648 243

The figure 25 summarises the results displayed in tables 11 and 13, where it shows the difference in *NPV* for 20 and 40 years. It appears from the figure that the added 20 years increases the *NPV* by a small margin.

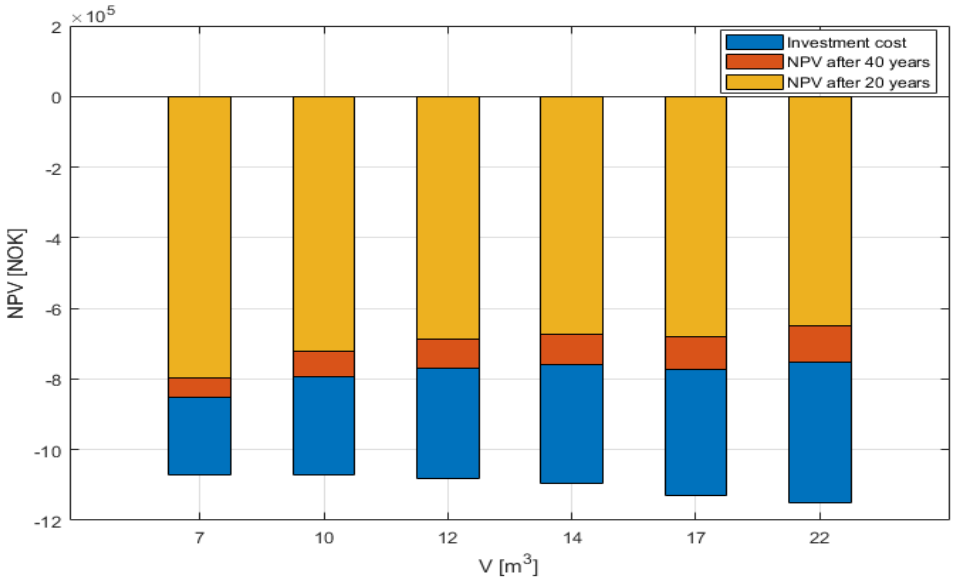

Figure 25: The difference in *NPV* after 20 and 40 years, along with the investment costs.

5 Discussion

The discussion will be separated into different sections. It starts of with a general discussion regarding the modelling approach, the system at hand, and the heat pump in section 5.1. In section 5.2 the deterministic and GA optimisation methods, as well as their strengths and weaknesses are discussed. The peak shaving and economic aspects from Case A will also be discussed in their respective sections. Section 5.3 is separated into general discussion and economic aspects, where the approach used in Case B, as well as the results from the simulations, will be discussed in depth.

5.1 General discussion

5.1.1 Evaluation of data

The method to detect and remove outliers explained in 3.2.1 should be valid, although they might not be as accurate as they could have been if a better statistic tool had been used to detect and replace the outliers. This could lead to a more accurate results from the simulations.

Figure 18 is an example, where it is a trend that the first hour during a day the energy consumption is higher than the remaining data. It is certainly possible that the energy consumption should look like this, but it should not be excluded that it is caused by outliers still being present in the data set. If it is not caused by outliers, it could indicate that the control strategy is less optimal than it could have been.

Another aspect that should be mentioned regarding the data set, is that all the data are treated equally, except for the outliers mentioned above. That is to say, the uncertainties from the measuring instruments were not taken into consideration, which might lead to inaccurate results. However, because the simulations conducted in this thesis has numerous assumptions and simplifications, it is assumed that said uncertainties would not make the results more accurate.

5.1.2 Modelling approach

Due to the limited time of this assignment, and only having basic knowledge of thermodynamics, fluid mechanics, and programming at the start of the project, the model was chosen to be as simple as it is. If more time had been available, a more complicated model could have been made. This could for instance entail a more analytic approach to evaluating the pumps and heat pumps. Some of the factors just mentioned could potentially improve the results as they are now. Besides, the tank is placed outdoors, where solar radiation and other weather phenomena may also affect the temperature gradient. However, despite all the assumptions and simplifications that are made in the model, it should still produce viable results, especially concerning overall trends.

Another factor that could improve the model, is if a different TES tank modelling approach had been taken. If a modelling approach had taken CFD into account, for instance, it would have yielded a much better representation of the thermocline, as it would consider complex physical phenomena. It would thus increase the accuracy of the

model, as it would grant a better depiction of the energy stored in the tank. However, this approach would have taken significantly longer to compute, and, perhaps more importantly, it would be comparatively much harder to create the model. The choice of tank modelling approach speculated to have had a substantial impact on the results, as the MB modelling approach negates a notable amount of factors that affect the temperature gradient inside the tank.

Another aspect that might have increased the accuracy of the model, would be to explicitly consider how the use patterns and the HVAC system affects the heat consumption. However, as the results are based on historical data, it is presumed that these factors are implicitly regarded.

5.1.3 The system

The system is designed for a supply temperature of 80°C and return at 60°C, which has some negative consequences for the system. Firstly, the losses in the tank are increased due to the increased ΔT between the water stored in the tank and the outside temperature. The heat pump will also be less fit for the system, as it has a maximum output temperature of 50°C. However, as mentioned in chapter 3.1, the temperatures are often lower than the design temperatures, which leads to the heat pump performing better than what the design conditions would suggest. The possibility of storing more energy in the tank would also be there, as the ΔT could be increased by 20°C if the temperatures of the system were changed to 60/40, and the upper limit in the tank is kept at 80°C.

The peaks that are produced during winter are extremely hard to subdue, as they sometimes appear in close sequences. One way to improve the peak shaving during the winter could be to increase the maximum temperature in the tank. Where the upper limit for the TES tank could have been increased for example up to 95°C rather than 80°C. This would result in a $\Delta T = 35$°C, which in return could give the tank a higher possibility to reduce the peaks by increasing the energy storage of the tank. However, one prominent drawback would be that the losses would increase, as the ΔT between the water and the ambient temperature would increase.

The TES tank is installed in the system to act as a pilot project to evaluate the feasibility to use such a strategy to reach NTNU's short-term climate goals. It will be used to analyse if it investments like this could be beneficial on a larger scale. Thus, the price of this installation is most likely higher than what it would be acceptable if it was done on a larger scale, or if it had been installed in another system.

During summer months, when the heat demand of the building is low, and the TES tank is charged, the energy stored will likely end up as losses. However, in real systems, this can be negated by smart control strategies (i.e. discharge the tank before the summer, etc.), but the model used in this thesis is not designed to do this. This will result in larger losses (and thus less savings) than otherwise would have been the case. The GA might be "lucky" and find a solution that accounts for this.

The volume term subtracted from the energy component of the total cost during winter is dependent on ΔT between the water at the inlet and the outlet of the substation. This term is not calculated in the model, and it is assumed to

be equal to the measurements from the historical data. However, this will likely change when a TES tank is installed in the building, as this changes the heat consumption of the building. This will cause this part of the price to be erroneous, where it would probably sometimes be higher, and sometimes be lower. It should therefore be considered as a rough estimate to what the actual price should have been.

5.1.4 Heat pump

The data provided by NTNU regarding the heat pump was insufficient – the data sheet lacked detailed information about the *COP* factor, and how it changed with the temperature; while the temperature sensor at the input of the heat pump lacked historical data. The electric input was given as daily values, whereas the rest of the data was measured hourly. Therefore, doing any investigation of how the heat pump impacted the system would be less accurate. All this considered, it is omitted from the analysis conducted in this report. However, the impact it has working in tandem with the TES tank is still interesting, and it has an important role in the system.

It is probable that the system, including the TES tank and the heat pump, could be able to sustain the local heating systems during the summer months, without the need to buy any heat. However, if there is a peak which the system is unable to shave, it might not affect the thermal comfort in the building if neither the heat pump nor the tank is able to supply the needed energy.

5.2 Case A

5.2.1 Deterministic optimisation

Table 6 indicates that it is economically favourable to consider a weekly consumption of heat with this model, given that the tank is required to discharge completely, unlike for daily values. This would save $\sim$1 350NOK compared to the daily consideration. This was as expected, as a longer period should make the system more likely to be prepared for the peak loads. The daily considerations could also discharge the tank a day prior to a peak, and therefore not be able to adequately shave the highest peaks. On the other hand, when considering a weekly period, $\dot{Q}_S$ will stay the same for a week instead of a day, which may have an impact on the power price if the week spans over two months. This occurs in February and March 2018, where February had a large peak at the end of the month, and said week spanned into March, where the $\dot{Q}_S$ appropriate to shave the peak in February is not appropriate for the first week in March. This can be seen in the figure 19 and in appendix F.1. It is also the reason why the peak shaving conducted on the weekly consideration was larger than the ones for the daily consideration, which can be seen in figure 17. However, this should not affect the results too much, as the peak in March is quite high. This might also occur during other months with lower peaks where it is harder to detect. In a worst case scenario, this might lead to the fact that the power price for the next month is larger than necessary. Despite this, the weekly consideration still yielded the best results, although the difference equated to only about 1.33%. Even though this flaw was discovered, it was chosen not to be dealt with, as the results were already adequate and it would require a significant amount of time to improve the model.

In general, taking a longer time period into account would grant better results, as seen when comparing daily and weekly considerations in table 6. This is, however, best achieved in a retrospective view, as the weather forecast is limited to ten days. With the facts mentioned above in mind, finding an optimal time period to consider can be difficult, as different factors are important and may have more or less of an impact on what the optimal time period is. There might be a different time period that would be optimal in terms of both being realistic regarding the time span as well as providing decent results. In the future, it might be beneficial to use the daily consideration, in case the pricing of district heating becomes dependent on the current consumption. This would lead to charging during the night and discharging during daytime to be the most profitable method. This change of pricing is however not announced, making this mere speculations.

5.2.2 Genetic algorithm

The reason for making a GA is twofold. Firstly, it might prove useful for the project, as it might yield different results than the optimisation conducted in case A1. Secondly, learning to build and use a GA is viewed as invaluable knowledge to possess due to its adaptability in different situations. Even though the difference in price in case A1 and case A2 is negligibly small, the time used to build, debug, and run the GA is still deemed appropriate, as the learning outcome of this part of the project has been large.

The results from the GA were disappointingly small compared to the results from case A1; the increase in price was almost negligibly small. This might be due to the output $\dot{Q}_S$ from the optimisation conducted in case A1 were used as input parameters in the algorithm to try to optimise the price difference; where $\dot{Q}_S$ might have reached a local optima close to the global optimum when price is considered even before the GA was run. This is seen by the fact that, for both the daily and weekly consideration, the EPPs in the figures 15 and 16 converge relatively quickly. Another explanation for this might be that, as the original $\dot{Q}_S$ was multiplied by a random number in the range [0.7,1.3], it might have resulted in a $\dot{Q}_S$ that was close to the optimal $\dot{Q}_S$ by chance.

The EPP for the weekly consideration displays a more erratic pattern than the daily consideration, where the maximum drops after a few generations. This might be explained by the nature of randomly generated numbers – it is possible, albeit statistically improbable, that this occurs. Firstly, the chromosomes chosen to be reproduced – or be chosen to be present in the next generation without crossing or mutating – are chosen probabilistically, which means that even the unlikely outcomes might occur. Secondly, the chromosomes that scored well on the fitness function might be chosen for mutation, where the mutation might cause the chromosome to perform worse in the next generation. If the GA had been ran more than once, results like these might be avoided. This was not done, as the results from the GA are adequate, and it is not the evaluation of the GA in itself that is objective of this thesis.

Another aspect of the GA concerns the validity of its results. For instance, how can it be verified that the GA explores the entirety of the feasible region? The script tries to evade this issue by setting the crossover rate p_c at 0.35, which causes approximately 35% of the chromosomes to produce offspring – this leads to a larger fraction of the feasible region to be searched. Besides, it appears from the figures 15 and 16 that the optimisation converges

relatively quickly, leading to the assumption that 200 generations are adequate, at least for this population size. However, the daily simulations found its maximum value after 192 generations, although it appears from figure 15 that the changes in price were insignificant. The mutation rate p_m was also set at 0.01 (or 1%), to reduce the possibility of generating noise that obfuscate the results, while also being large enough to create random variation in the population that might or might not be beneficial. With the specified p_m, approximately 1% of the total number of genes are mutated at each iteration, creating variation within the generation. The range [0.7,1.3] could have been chosen to be larger, so that a larger feasible region would be searched. This might have produced a better result. The same can be said for the constraints set to limit the maximum $\dot{Q}_S$ to 750kW – if this had been chosen to be larger, the feasible region would in turn be larger, and perhaps yield a better result. Lastly, the number of decimal points were set to three, as this results in $\dot{Q}_S$ having the precision of 1W; this precision seems small enough to cover a large part of the feasible region (especially during periods where the load is small). As discussed in the previous section, the model uses several approximations and simplifications, and anything smaller would not have made any sense. Practically, maybe it could have sufficed with two, or maybe even one decimal.

20 chromosomes was chosen instead of a larger amount to limit computation times, while also not compromising on the amount of solutions at each generation. However, as can be observed in figure 16, and perhaps especially in figure 15, the diversity of the population disappears early, and the maximum at each generation converges quickly to the final value. This might indicate that the amount of chromosomes should have been increased.

The largest downside of using a GA is reproducibility and predictability. Due to it being highly stochastic in nature, with several randomly generated numbers during the course of a generation, executing the GA several times might yield different results, where they might or might not coincide. Theoretically, the results will converge asymptotically towards an optimal solution, but when this occurs is not predictable, so predetermining the required amount of generations is impossible. Thus, a more optimal solution might exist that could have been found; either by running the GA several times, or if it had been run for a longer period of time. Besides, the GA written for this project was a very simple model, and it is reasonable to assume that a more complex GA would have provided better results. This could have been carried out by e.g. using a different approach than the roulette wheel approach, or by using a different scheme for scoring the chromosomes than Π_{diff}.

5.2.3 Peak shaving

Figure 17 demonstrates how much the maximum peaks for a given month is reduced. Especially the summer months have had their peaks shaved significantly, with the load during the summer of 2017 being cut by more than half. As seen in figures 18 and 19, the peaks are considerably harder to shave in 2018 compared to 2017. This is due to the peaks being higher and lasting for longer time periods, caused by longer periods of cold weather. The peaks in 2017 are quite tall, but does not last long, relatively, and are therefore possible to reduce efficiently. Simultaneously, the district heat consumption is far lower during the summer of 2018, due to a very consistently warm summer. This may be part of the explanation of why figure 17 shows that the peaks from 2017 in general are smaller than in 2018 in the beginning of the year, but higher during summer, autumn and the start of the winter.

It is important to note that the loads in figure 20 only represent the load shift on an average day over the two year period, and the actual usage may not look like this on a randomly selected day. This holds especially true during the summer part of the plot, as this is defined by Statkraft Varme AS as lasting from March to October; these months have a wide range of outdoor temperatures (and therefore heating needs) and building use patterns – for instance like summer vacation, where little to no activity is assumed. However, it should still be able to say something about the general trends during these periods. It specifically shows that the model is well equipped to smooth out the loads, where it, on average, shifts the loads from morning to evening and night.

Figure 21 shows the difference between the energy consumption before and after the TES tank was added to the local heating system of the NHL building. As stated in chapter 4.1.3, the base load has increased, while the peak load has been decreased, when comparing before and after the TES tank was installed in the system. Ideally, the energy consumption should be reduced as much as possible on the left hand side of the curve, as this would indicate a successful load shift; however, the results are very much acceptable. This reduces the costs of heating at the NHL, which, in turn, reduces the payback time on the investment.

The shape of the ET-curve from after the simulations in figure 22 is narrower than the ET-curve from before. This indicates that the loads at specific temperatures have moved towards the average value. This is presumably because that the values below a certain level have been used to charge the tank, resulting in the load at a certain temperature to be increased; while the values above a certain level have been shaved, thus moving closer to the average. It also appears that the highest peaks during the two-year period are flattened out, where the maximum load present after is $\sim$650kW, down by almost 100kW. This is an indication that the system is working as anticipated.

As mentioned in chapter 4.1.3, the efficiencies of the tank was 96.3% and 88.8% for the daily and weekly consideration respectively. The efficiency of the weekly consideration is noticeably lower, by almost 10%. This is because the tank is idle for longer periods of time without being emptied, causing the energy stored in the tank to exit through the walls rather than the pipes. It may also indicate that the period at which the efficiencies were calculated at, was too long. Perhaps several cycle efficiencies would be better to calculate, and present a more realistic efficiency. In either case, these efficiencies are very optimistic, as they do not consider the temperature degradation of the heat in the tank, as was mentioned in chapter 2.3.4. However, as they are calculated the same way, they should still be comparable and be used to evaluate the tank's performance in relation to each other, even if they are both wrong.

It can be argued that efficient energy usage is more important than economic gains, as the economic aspects are not the main objective of the project. Besides, the difference in price between the two scenarios is only $\sim$1.33%. This is also in accordance with NTNU's climate goals, where better energy efficiency is one of the main ways to reduce the amount of energy that is consumed. It is also assumed that, if smarter control strategies are utilised than what is used in the simulations, the difference in the yearly savings can be reduced.

On a side note, although this is not the purpose of this project, it is speculated that a reduction in peak loads at NHL reduces the strain on Statkraft Varme AS' heating grid – it is presumed that most office and industrial buildings have

a peak generally around the same time, and that these peaks propagate upwards in the grid. A reduction in these might cause a reduction in Statkraft Varme AS' own peaks. However, a single building might not necessarily have a large impact on the district heating grid. Further work can be conducted to confirm or contradict this assumption.

5.2.4 Economic analysis

Figure 20 indicates that the daily values shift the load more significantly in comparison to weekly values. However, the weekly considerations cuts the maximum power consumption slightly more than the daily ones, causing the price difference between them to be $\sim$1 400NOK, or $\sim$700NOK per year. Although it represents 1.4% of the total savings for this building, it represents only a small fraction of what NTNU spends on heating on a yearly basis. On the other hand, if this is the case for several buildings, it might add up to a significant amount in the long run.

The TES tank that is installed at the NHL building was specifically made for that system (in contrast to an off-the-shelf tank). This causes the *PP* and the *NPV* to be respectively much higher and lower than what is favourable. However, as this is not a project where the maximisation of returns is the main goal, this is not necessarily a problem.

The *NPV* indicates that the investment has a total loss of $\sim$768kNOK. The main reason of the economical losses is due to the investment being this large, if the installation of the system would have been simpler, without upgrading the heat central etc., it might have been a better investment, and maybe it would even have yielded a positive *NPV*. In addition, the investment costs and operational costs of the tank are proportional to each other for this simulation, therefore a lower investment cost would lead to a lower operational costs. However, it should be noted that this would not necessarily be the case in a real-world scenario.

5.3 Case B

5.3.1 General discussion and tank performances

As in case A, the tanks used in case B are also custom-made. The implication of this is that the tanks could presumably be cheaper if an off-the-shelf tank had been considered. The investment costs and the geometries of the tanks mentioned in chapter 3.4 are rough estimates provided by Martin Sæterbø, and may not necessarily reflect the actual prices of the tanks.

The losses due to the geometries of the tanks are some of the the most prominent sources of error, as all the tanks are considered to be the same height. This leads to the fact that the larger the tank, the less the ratio between the volume and the height becomes. As can be seen from equation (2.3), the losses are proportional to the tank's area. The largest tanks should therefore systematically perform better, as the assumptions about the height works in favour of them. This is demonstrated by figure 23, where the largest tanks performs the best, and the smallest ones has the lowest efficiency. Real tanks, however, presumably have different aspect ratios between the height and the volume than assumed in this report, and it is not necessarily true that the largest tanks performs better than smaller ones in this system.

Despite what was mentioned in the paragraph above, some of the bigger tanks does not perform as well as some of their smaller counterparts. For instance, in figure 23, it appears that the $17m^3$ tank performs better than both the tanks directly smaller and bigger, for the daily consideration. As mentioned in chapter 2.3.4, the spherical and barrel-shaped tanks has the largest heat capacities, and the spherical tanks has the best efficiencies. The $17m^3$ tank has the aspect ratio between the height and the width closest to one, which might be the reason why it has the best efficiency when considering the daily periods.

It is true for case B as for case A that the daily consideration had better efficiencies than the weekly consideration, though they seem to converge as the tank size increase. For the daily consideration, although it is not directly apparent from figure 23, the efficiency for the $22m^3$ tank decreases in comparison to the $17m^3$ tank. As this is the largest tank tested in the simulation, it is not possible to extrapolate that this might be a trend for larger tanks, but it is assumed that a larger tank will be less and less suited for the system, as more and more of the tank volume becomes idle. It is possible that the $22m^3$ tank becomes so large that it is unfit for the system, but the evidence to support this is questionable at best. For the weekly consideration, however, the efficiency only increases with the tank volume. It is presumed to stem from it behaving more like a weekly TES than a diurnal TES.

As seen in figure 24, the change in size has a significant impact on the reduction in power peaks. Generally, the bigger tanks reduce the peaks more, especially the $22m^3$ tank. During the summer months, the difference in peaks are not that considerable, however, during the winter, the difference in for example in February 2018 is at around 60kW between the largest and the smallest tank. The largest difference was in May 2017, where the best tank shaved the peaks with almost 100kW more than the worst. There are two main exceptions, namely July and September 2018. In July 2018, the best performing tank was the largest, however, the second best was the smallest, which can be seen in appendices F.4 through F.6. This seems to stem from the $7m^3$ tank being unable to shave the peaks the week prior as much as the other tanks, and therefore having more energy stored in the beginning of the week. This leads to it being able to shave this peak decently. In comparison, the tank with a volume of $12m^3$ discharges to a higher degree the week prior, and is therefore unable to shave the peaks as much as the smallest one. The biggest tank is able to shave all the peaks better. The $\dot{Q}_S$ lingers from August on to September 2018 for the $12m^3$ tank, as the highest peak at the end of August leads to an unnecessary high $\dot{Q}_S$ in September. This can be seen in appendices F.2 and F.3. It is assumed that this is also the case for the remaining tanks in case B, where this is presumed to be the reason for the same level of peak shaving by the different tanks in this month.

There are also other aspects to take into consideration when deciding whether a change of size is feasible or not. One such factor is whether there is space to install a bigger tank, and if it would have a negative impact on the comfort of the building, by for example covering an office with shadow. However, these aspects are considered of secondary importance, after the technical and economical aspects.

5.3.2 Economic analysis

One way to improve the reduction of peaks can be achieved by adding a larger TES tank, as a larger tank will have an increased capacity. Some negative consequences of increasing the tank size are an increased charging time, as well an increment in thermal losses. However, as mentioned in chapter 3.4, the charging time is assumed to be equal to one hour, as it charged more than the pump can deliver only once during the two year period. However, as discussed above, if the tank is charged to its maximum capacity before a period with low consumption, the losses will be much larger than necessary. This holds especially true for the larger tanks, as they have more energy to lose to the surroundings.

One important factor is whether the increased volume is usable or not – if the tank is unable to either charge or discharge fully, for instance, the increased volume will not amount to anything. Besides, as mentioned in chapter 2.3.4, the increased volume leads to more losses, and if the size is too large, the added losses negate the benefits of including the tank to the system. The *NPV* and *PP* are indicators of this, as both of these take the losses into account, as well as the investment and operational costs. Tables 11 and 12 seems to indicate that this point is not yet met, as they increase and decrease, respectively, by increasing the volume. However, as the effectiveness of the tank and the second-law efficiency are not considered, this analysis is not in-depth enough to be able to conclude that any of the tank sizes represent an optimal volume for this system.

The TES tank that yielded the best *NPV* and *PP*, was the one with an internal volume of $22m^3$. The $17m^3$ tank, however, performes worse than both the $14m^3$ and $22m^3$ tanks. The efficiency of the tank, as seen in figure 23, is in-between the efficiencies of the $14m^3$ and $22m^3$ tanks. This leads to the assumption that it may be caused by it not being able to generate a price difference large enough to cover both the increased capital costs, as well as the increased losses in the tank. It may also be caused by how the $17m^3$ tank handles the charge and discharge sequences, as the tank demands more energy but may discharge at times less likely to generate a difference in price.

The *NPV* assumes that the tank and none of the equipment listed in table 4 have any residual value other than potential costs of scrapping the tank at the end of it's economic life expectancy. This yields an inaccurate *NPV*, as at least some of the costs listed in the table are presumed to be recoverable at the end of the life of the tank.

The *NPV* of the investment is negative, however, from an environmental aspect, the investment might still be advantageous. With the model NTNU uses for the CO_2 emissions from different energy carriers, which assumes that the emissions from district heating and electrical power is equal, it is beneficial to use the heat pump rather than the district heating. Similarly, storing the energy with the least CO_2 emission could be equally important, which could be done by charging the tank with the heat pump rather than the district heating. This means that, although the *NPV* is negative, the investment might be beneficial in the long run.

As presented in table 12, the *PP* of all the tanks are all greater than the initial economic life expectancy assumed in this report, where the largest one has a *PP* of approximately 31 years. This indicates that the tanks will not be

profitable before the end of its life. However, as stated in chapter 2.8.4, a TES tank life expectancy can be more than 40 years, which causes all the tanks having a volume of $14m^3$ or larger to be able to be profitable, according to this method, if a longer economic life expectancy is allowed in the model. Furthermore, the *PP* method has some important flaws, as it neglects the time value of money and the rent of investment. This is evident if the *NPV* is considered for 40 years, presented in table 13, where they are only marginally better than the *NPV*s in table 2.8.4 despite having a positive net income for another 20 years. The price differences are presented in figure 25.

This simulations assumes that the pricing of district heating would stay the same for the next 20 or 40 years, however, it is likely that the pricing scheme could change during this period, especially considering that a change like this occurred in 2018. Changes in the pricing could likely impact the analysis conducted in this project. However, the installation of at TES tank could still be beneficial, as for example one speculated change is that the price would be set hourly, which would most likely make the peak loads an even greater expense. If this was the case, having a TES tank for diurnal energy storage would be beneficial.

6 Conclusion

The model created for this thesis worked well, where it managed to shave the peaks adequately, despite the issues concerning the $\dot{Q}_S$. However, it is possible to avoid this error by simulating for daily values rather than weekly. The GA improved the results from the deterministic simulations slightly, however the difference was less than expected. It is considered a product, and is delivered alongside this bachelor thesis. It can easily be adapted and applied to other buildings and other scenarios if it is given more detailed input data, especially as a first analysis in the planning phase of a similar project. The usage of it in this thesis can be considered as a proof of concept.

In case A, two tank control schemes are simulated, where peak shaving is conducted on a daily and weekly basis. Furthermore, it is divided into two parts, where two different optimisation strategies are tested, where the first one optimises the peak shaving level with a deterministic optimisation approach, while the second strategy optimises the price difference before and after the tank was installed, and it utilises a genetic algorithm optimisation approach.

From the simulations it can be concluded that the tank is shaving the peaks in an adequate way, where the highest peaks in the data set are reduced by $\sim$100kW in February 2018, the largest cut was around 175kW in May 2017, and the average reduction per month was 100kW, all in the weekly consideration. There is a significant difference between the peak load before and after the simulations are conducted for every month. The daily considerations did in general shave the peaks more than the weekly, however the results in terms of price turned out to be similar, with a total difference of 1.33% for case A. The total *NPV* for the project was -775kNOK, while the efficiencies were 96.3% and 88.8% for the daily and weekly consideration respectively. After evaluating the efficiency and price difference, the daily consideration was the better strategy, as it was more efficient, and had an *NPV* that was almost as negative. This is in accordance with NTNU's climate goals for the near future, and might help reduce the total energy consumption, especially if it is used in tandem with the heat pumps.

In case B, different tank sizes were simulated and compared with each other, where the net present value, payback period, and tank efficiency were taken into consideration. The results from the simulation indicated that a larger tank would be more beneficial, where the efficiency increased with the expansion of the tank volume. The *NPV* and *PP* increased and decreased respectively when the tank volume was expanded, except the 17m^3, which yielded worse result than both 14m^3 and 22m^3 for weekly. However, when the efficiency is taken into account, the 17m^3 for the daily consideration, and 22m^3 for the weekly consideration, seems like the most optimal tank sizes for the respective control strategies, but the assumptions might be biased towards the larger tanks. Furthermore, the simplifications and assumptions used in this report contribute to making it unclear whether these tanks would be better fit for the system or not.

7 Future work

The model created for this project uses several simplifications and assumptions. Therefore, it might be beneficial to increase the complexity of it to attain a better overview of the dynamics of the system. This could e.g. be by using a different program to simulate the system, or by including more aspects of the local heating system, such as the heat pumps, heat exchangers, a more complex tank model, and pumps, as well as a more in-depth investigation of the load. Furthermore, an optimal control strategy could be developed for the tank. Lastly, it may be interesting to investigate other methods to recycle or produce energy within the building, be it electric or in the form of heat.

References

[1] NTNU Eiendomsforvaltningen. NTNUs miljøambisjon, 2011. https://www.ntnu.no/documents/10137/323403/NTNU_Milj%C3%B8ambisjon.pdf/9d9fe7cd-02d3-4342-beca-9af23afac4af, [Accessed: 22.01.2019].

[2] NTNU. Ambisjoner og fakta. https://www.ntnu.no/miljo/miljoambisjon, [Accessed: 22.01.2019].

[3] May Brit Leirtrø Røstad. Slik kan campus få smarte energiløsninger, 2018. https://www.ntnu.no/campusutvikling/2018/campus-smarte-energiloesninger, [Accessed: 01.05.2019].

[4] Michael J. Moran, Howard N. Shapiro, Daisie D. Boettner, and Margaret B. Bailey. *Principles of Engineering Thermodynamics*. John Wiley and Sons, Ltd., 8th edition, 2015. SI version.

[5] Zhiwen Ma, Greg Glatzmaier, Craig Turchi, and Mike Wagner. Thermal energy storage performance metrics and use in thermal energy storage design. pages 1–6, 05 2019.

[6] İbrahim Dinçer and Marc A. Rosen. *Thermal Energy Storage. Systems and Applicatons*. John Wiley and Sons, Ltd., 2nd edition, 2011.

[7] P. S. Ghoshdastidar. *Heat Transfer*. Oxford University Press., 2nd edition, 2012.

[8] R. Rudramoorthy and K. Mayilsamy. *Heat transfer : theory and problems*. Pearson, 1st edition, 2005.

[9] Vinod Nirale. Thermal analysis of composite slab, cylinders. *International Journal of Research in Advent Technology*, 3(8), 2015.

[10] A. Karim, A. Burnett, and S. Fawzia. Investigation of stratified thermal storage tank performance for heating and cooling applications. *Energies*, 11(5), 2018.

[11] Liang Wang Yong Sheng Zheng Yang, Haisheng Chen and Yifei Wang. Comparative study of the influences of different water tank shapes on thermal energy storage capacity and thermal stratification. *Renewable Energy*, 85:31–44, 2015.

[12] Olivier Dumont, Carolina Carmo, Rémi Dickes, Emeline Georges, Sylvain Quoilin, and Vincent Lemort. Hot water tanks : how to select the optimal modelling approach? In *Conference CLIMA 2016 (du 22 mai 2016 au 25 mai 2016)*, 2016.

[13] Kui Wang, Marco A. Satyro, Ross Taylor, and Philip K. Hopke. Thermal energy storage tank sizing for biomass boiler heating systems using process dynamic simulation. *Energy & Buildings*, 175:199–207, 2018.

[14] Jørn Stene. Varmepumper : bygningsoppvarming. Technical report, SINTEF, Trondheim, 1997.

[15] Jørn Stene. Varmepumper : grunnleggende varmepumpeteknikk. Technical report, SINTEF, Trondheim, 2001.

[16] Maurice Stewart. *Heat exchanger equipment field manual : common operating problems and practical solutions*. Focal Press, New York, 2013.

[17] Mohammed Al Arfaj, Nasser Al Mulhim, Abdullah Al Mulhim, and Ahmed Al Naim. Design of cross flow heat exchanger using performance charts. *International Journal of System Modeling and Simulation*, 3(2):1–6, 2018.

[18] Abdur Rehman Mazhar, Shuli Liu, and Ashish Shukla. A state of art review on the district heating systems. *Renewable and Sustainable Energy Reviews*, 96:420–439, 2018.

[19] Regulering av prisen på fjernvarme. ECON-rapport (online), 2010.

[20] Norsk Fjernvarme. Energikilder trondheim 2017. `http://www.fjernkontrollen.no/trondheim/`, [Accessed: 04.02.2019].

[21] Statkraft Varme AS. Tekniske bestemmelser for fjernvarme kundesentraler og innvendig røranlegg., 2017.

[22] Statkraft Varme AS. Data til bruk i breeam-sertifisering for kunder av statkraft varme i trondheim - 2018, 2018.

[23] Fredrik Wernstedt, Paul Davidsson, and Christian Johansson. Demand side management in district heating systems. In *Proceedings of the 6th international joint conference on autonomous agents and multiagent systems*, AAMAS '07, pages 1–7. ACM, 2007.

[24] Vittorio Verda and Francesco Colella. Primary energy savings through thermal storage in district heating networks. *Energy*, 36(7):4278–4286, 2011.

[25] Statkraft Varme AS. Energiguiden – ditt verktøy for lavere energikostnader. `https://www.statkraftvarme.no/globalassets/2-statkraft-varme/statkraft-varme-norge/bedrift/energiguiden-kort-brukermanual.pdf`, [Accessed: 05.03.2019].

[26] Roger Parkyn. Duration (CDF) Plot, 2013. [MATLAB-script]. version 1.9.0.0. `https://se.mathworks.com/matlabcentral/fileexchange/27817-duration-cdf-plot`, [Accessed: 05.03.2019].

[27] Rolf Ulseth and Jacob Stang. *SIE 1045 Energisystemer : Del 3 : Vannbåren varme : systemer og egenskaper.*, chapter 5. Mengderegulerte varmesystemer - dimensjonering av rørnett. NTNU, 2000.

[28] Ashok D. Belegundu and Tirupathi R Chandrupatla. Preliminary concepts. In *Optimization concepts and applications in engineering*, pages 1–45. Cambridge University Press, 2nd ed. edition, 2011.

[29] Mitsuo Gen and Runwei Cheng. Foundations of genetic algorithms. In *Wiley Series in Engineering Design and Automation*, pages 1–41. John Wiley & Sons, Inc., Hoboken, NJ, USA, 2007.

[30] K. D. M. Harris, R. L. Johnston, and B. M. Kariuki. The genetic algorithm: Foundations and apllications in structure solution from powder diffraction data. *Acta Crystallographica Section A*, 54(5):632–645, 1998.

[31] Will Tipton and Richard Hennig. GASP: The genetic algorithm for structure and phase prediction, 2015.

[32] Jenna Carr. An introduction to genetic algorithms, 2014.

[33] Energiloven. *Lov om produksjon, omforming, overføring, omsetning, fordeling og bruk av energi m.m.* (LOV-2018-05-25-21 fra 01.01.2019), 1990. `https://lovdata.no/dokument/NL/lov/1990-06-29-50`.

[34] Statkraft Varme AS. Prismodell. https://www.statkraftvarme.no/produkter-og-tjenester/Prismodell/, [Accessed: 06.02.2019].

[35] Statkraft Varme AS. Ny modell for pris på effekt i trondheim, 2018. https://www.statkraftvarme.no/om-statkraftvarme/presse/nyheter/ny-modell-for-effekt/, [Accessed: 06.02.2019].

[36] Statkraft Varme AS. Fjernvarmetariff bt1v til næringskunder i trondheim.

[37] Nord Pool AS. About us. https://www.nordpoolgroup.com/About-us/, [Accessed: 08.04.2019].

[38] Nord Pool AS. Market data, 2019. https://www.nordpoolgroup.com/Market-data1, [Accessed: 08.04.2019].

[39] Geir Eggen and Geir Vangsnes. Heat pump for district cooling and heating at oslo airport, gardermoen, 2005. https://www.sintef.no/globalassets/project/annex29/installasjoner/gshp_gardermoenhp_no1.pdf, [Accessed: 30.04.2019].

[40] Kjell Banken. *Innføring i bedriftsøkonomi*. Cappelen akademisk forl, Oslo, 1999.

[41] Jaclyn Kinson. Energy storage strategies for the university of new hampshire. a feasibility analysis of energy storage opportunities on the durham campus, 2017.

[42] Will Kenton. Net present value, 2019. https://www.investopedia.com/terms/n/npv.asp, [Accessed: 24.04.2019].

[43] Julian Kagan, 2019. https://www.investopedia.com/terms/p/paybackperiod.asp, [Accessed: 12.05.2019].

[44] Øystein Engan. Staff Engineer at Campus Services Section. Communication per e-mail, 06.02.2019.

[45] Øystein Engan. Staff Engineer at Campus Services Section. Communication per e-mail, 24.04.2019.

[46] Cetetherm SAS. Cetetherm, cetetube. shell and tube heat exchanger. Datasheet, https://www.cetetherm.com/download/18.27bcc828167801b1d4f689/1544537855039/Cetetube%201811.pdf.

[47] Systemair. Air cooled heat pump. selected unit: Sysaqua 140. Datasheet, internal document.

[48] Grundfos X. Grundfos x. magna3 40-120 f, 2018. Datasheet, internal document.

[49] Brukermanual. vanntank, 2019. Datasheet, internal document.

[50] Martin Sæterbø. Teknisk leder at Skala Fabrikk AS. Communication per e-mail, 29.04.2019.

[51] Engineering ToolBox. Thermal conductivity of common materials and gases, 2003. https://www.engineeringtoolbox.com/thermal-conductivity-d_429.html, [Accessed: 09.04.2019].

[52] Engineering ToolBox. Polyurethane insulation, 2007. https://www.engineeringtoolbox.com/polyurethane-insulation-k-values-d_1174.html, [Accessed: 08.04.2019.

[53] Forbrukerrådet. Norske årsmiddeltemperaturer: I alfabetisk rekkefølge, 2015. https://fil.forbrukerradet.no/wp-content/uploads/2015/11/VP_2015_%C3%85rsmiddel_Alfabetisk.pdf, [Accessed: 08.04.2019].

[54] Thomas Murphy. This thermal house, 2012. https://dothemath.ucsd.edu/2012/11/this-thermal-house/, [Accessed: 08.04.2019].

[55] Trond Rikhard Haugen. Fagleder VVS. Communication per e-mail, 10.05.2019.

[56] Audun Grøm. Assistant professor. vice dean for engineering education at bachelor level at the IE Faculty Administration. Meeting, 03.05.2019.

[57] Martin Sæterbø. Teknisk leder at Skala Fabrikk AS. Communication per e-mail, 15.05.2019.

[58] Nord Pool Group AS. elspot-prices 2017 monthly nok, 2018. https://www.nordpoolgroup.com/globalassets/marketdata-excel-files/elspot-prices_2017_monthly_nok.xls, [Accessed: 21.01.2019].

[59] Nord Pool Group AS. elspot-prices 2018 monthly nok, 2018. https://www.nordpoolgroup.com/globalassets/marketdata-excel-files/elspot-prices_2018_monthly_nok.xls, [Accessed: 21.01.2019].

[60] Øystein Engan. Staff Engineer at Campus Services Section. Communication per e-mail, 25.02.2019.

[61] Eric Verner. Floating point number conversion, 2012. [MATLAB-script]. version 1.0.0.0. https://www.mathworks.com/matlabcentral/fileexchange/39113-floating-point-number-conversion, [Accessed: 20.04.2019].

[62] Mazemap AS. Kart og rom på NTNU. http://bit.ly/2TfqWAv, [Accessed: 05.03.2019].

Appendices

A Aerial image of the buildings analysed. Image edited from [62]

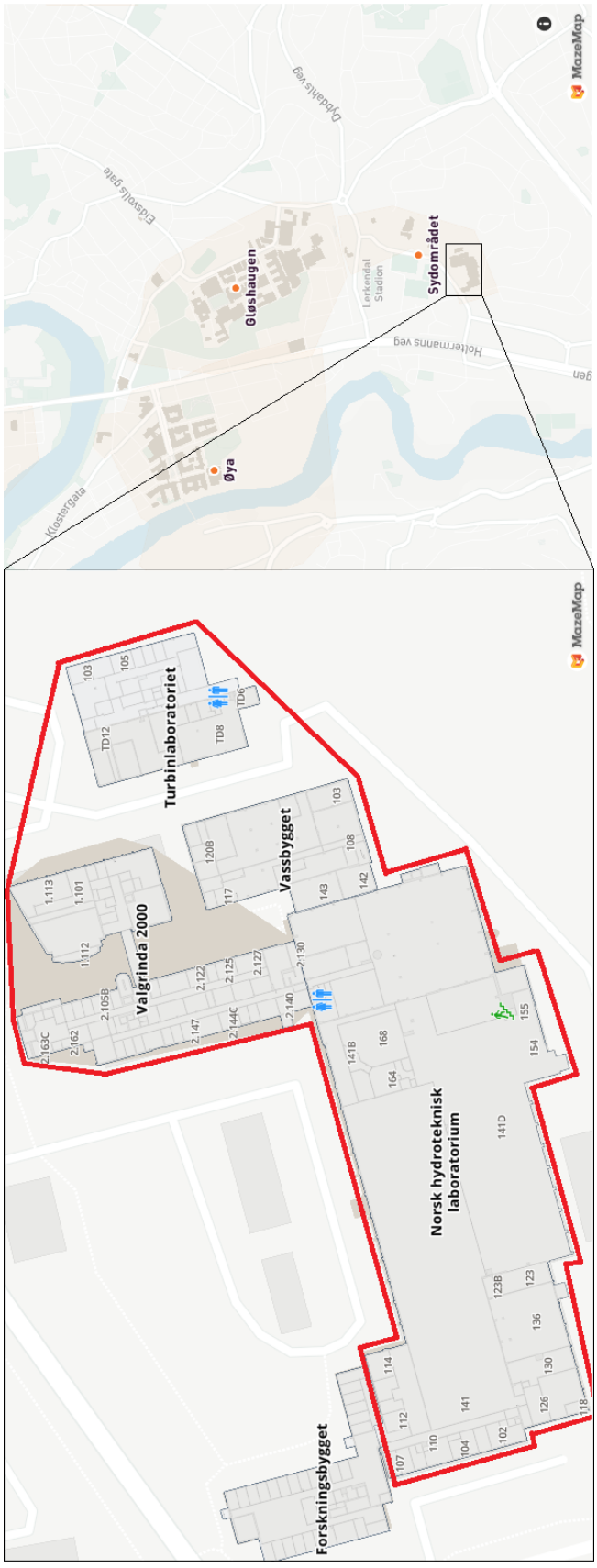

B Schematics of the system, provided by NTNU

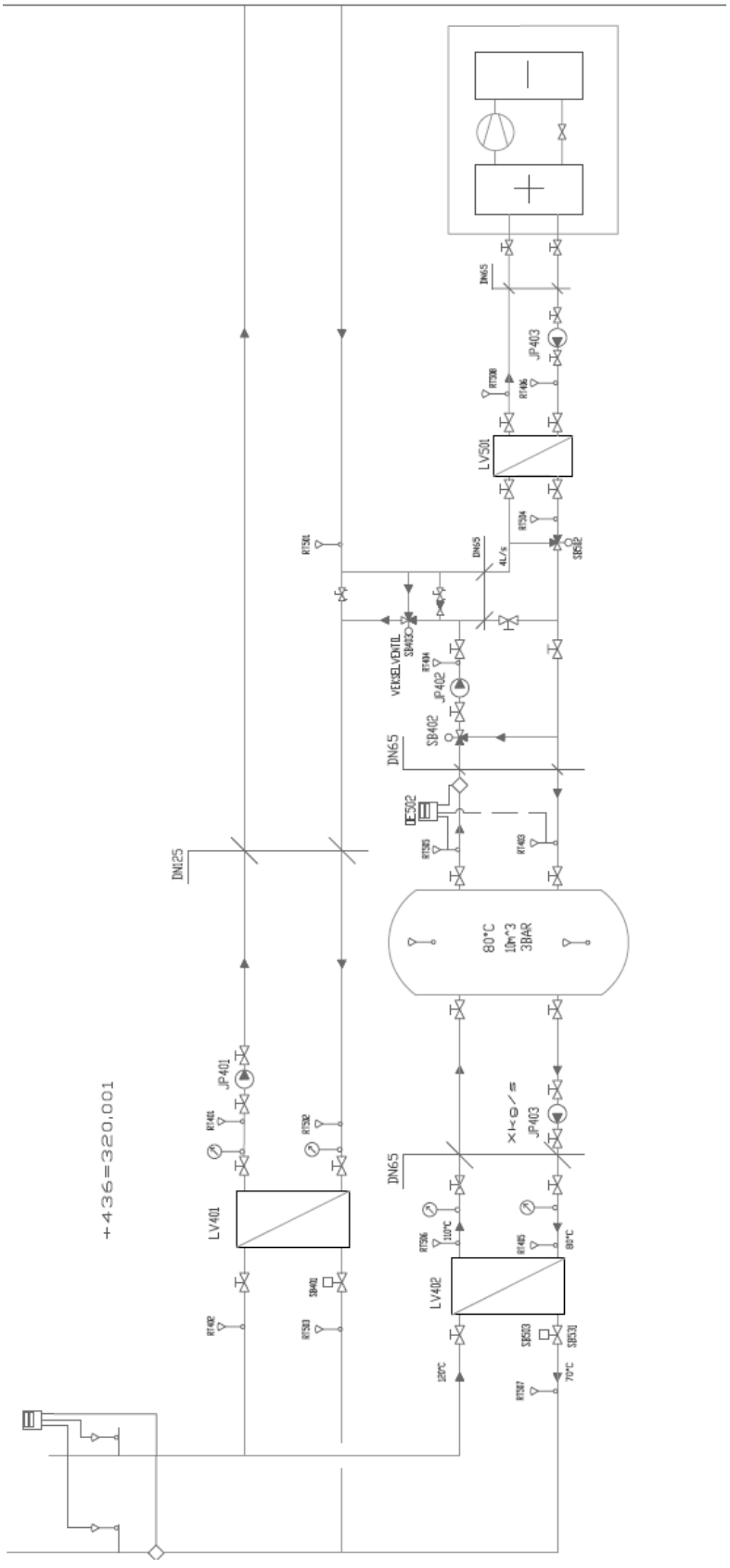

C MATLAB code for the simulations

```
clear, clc
tic
%% Controlers
% s == true used to test results from Genetic algorithm
s = true;
% Used to specify weekly or daily consideration
input_format = 'week';
%Counter is set to limit how many iterations the script does if an error
%occurs within the simulations, which would make the script loop
%indefinetly
Counter = 1000000;
% volume of the tank
V = 12;
Graphs = 1;             % 1 = plot graphs, 0 does not

%% Gathers data
load values_timestamps.mat
Constants


if s == true
    if strcmp(input_format,'week') == true
        load best_Q_S_weekly_run_2.mat
    else
        load best_Q_S_daily_run_3.mat
    end
end

%Qs = phenotype{11,15};

timestamp = values{:,11};
K = discretize(timestamp, input_format);
C = unique(K);

DeltaT = table2array(values(:,5));
ELs = table2array(values(:,13))';

% headers1 = {'Temperature', 'Volume_flow_rate', 'Q_VP','Elspot', 'Delta_T', ...
%     'Q_cleaned', 'Time', 'Season', 'avg_EL', 'time_day', 'Timestamp', 'day'};
% headers2 = {'Qtnk', 'FQ', 'FQ1', 'FQ2', 'Load', 'Delta_Qtnk', 'Temperature'};
```

```
% Output_table = cell2table(cell(24,7));
% Input = cell2table(cell(24,12));
% Output_table.Properties.VariableNames = headers2;
% Input.Properties.VariableNames = headers1;
%
% Output(1:length(C)) = struct('input', Input, 'Resultat', Output_table, ...
%     'Balance', zeros(1), 'Season', zeros(1), 'Q_S', zeros(1));

a = [eomday(2017, 1:12), eomday(2018, 1:12)]*24;
if strcmp(input_format,'day')
    slutt(1:length(C)) = 24;
elseif strcmp(input_format,'week')
    slutt(1:length(C)) = 24*7;
else
    slutt = a;
end

%% Simulation of the tank

for Z = 1:length(C)
    clear Variables
    if Z == 1
        k = 1;
        l = slutt(Z);
    elseif (strcmp(input_format,'day') || strcmp(input_format,'month')) ...
            || (Z <= 104 && strcmp(input_format,'week'))
        k = k + slutt(Z-1);
        l = l + slutt(Z);
    else
        k = (104*7*24)+1;
        l = 17520;
    end
    if Z == 1
        Qtnk_start = 0;
    else
        Qtnk_start = Qtnk(n);
    end

    Output(Z).input = values((k:l),:);
    Variables(:,1) = table2array(Output(Z).input(:,6));
    Variables(:,2) = table2array(Output(Z).input(:,1));
    [day, month, year] = ymd(table2array(Output(Z).input(:,11)));
```

```
    if s == true
        Q_S = Qs(Z);
    else
        Q_S = mean(Variables(:,1));
        if sum(Variables(:,1)) < 50
            Q_S = 0;
        end
    end

    FQ1 = zeros(1,length(Variables));
    FQ2 = zeros(1,length(Variables));
    Qtnk = zeros(1,length(Variables));
    Delta_Qtnk = zeros(1,length(Variables));
    Losses = zeros(1,length(Variables));
    counter(Z) = 0;
    f = true;
    while f
        counter(Z) = counter(Z) + 1;
        clear Losses Losses_1 Losses_2
        Movable = Variables(:,1) - Q_S;
        Movable_n = zeros(1,length(Movable));
        V_H = zeros(1,length(Movable));
        for n = 1:length(Movable)
            if n == 1
                Qtnk0 = Qtnk_start;
            else
                Qtnk0 = Qtnk(n-1);
            end
            if Movable(n) < 0
                Qtnk(n) = Qtnk0 + abs(Movable(n));
                FQ1(n) = abs(Movable(n));
                FQ2(n) = Variables(n,1);
                if FQ2(n) + abs(Movable(n)) > Q_S
                    FQ1(n) = Q_S - FQ2(n);
                    Qtnk(n) = Qtnk0 + FQ1(n);
                end
                if Qtnk(n) >= Qmax
                    Qtnk(n) = Qmax;
                    FQ1(n) = Qmax - Qtnk0;
                end
            else
                Movable_n(n) = Movable(n);
```

```
125                 Qtnk(n) = Qtnk0 - Movable(n);
126                 FQ2(n) = Q_S;
127                 FQ1(n) = 0;
128                 if Qtnk(n) <= 0
129                    Qtnk(n) = 0;
130                    FQ2(n) = Variables(n,1) - Qtnk0;
131                 end
132             end
133             V_H(n) = Qtnk(n) / (rho * C_P * DeltaTemp) * 3600;
134             h = V_H(n)/(Area);
135             Losses_1(n) = (Tmax - Variables(n,2))/U_1*h;
136             Losses_2(n) = (Tmax - Variables(n,2))/U_2;
137             Losses(n) = (Losses_1(n)+Losses_2(n))/1000;
138             if Qtnk0 > Qtnk(n)
139                 Delta_Qtnk(1,n) = -(Qtnk0 - Qtnk(n));
140             else
141                 Delta_Qtnk(1,n) = Qtnk(n) - Qtnk0;
142             end
143             if Qtnk(n) >= Losses(n)
144                 Qtnk(n) = Qtnk(n) - Losses(n);
145             else
146                 Losses(n) = Qtnk(n);
147                 Qtnk(n) = 0;
148             end
149         end
150         if s == false & ((max(FQ1 + FQ2) > Q_S) & counter < Counter)
151             Q_S = Q_S * 1.01;
152         elseif s == true | sum(Variables(:,1)) == 0 | counter(Z) >= Counter |
                ...
153                     ((((Qtnk_start + sum(FQ1) - Qtnk(n) - sum(Losses))...
154                     > sum(Movable_n) - 0.001) | ((Qtnk_start + sum(FQ1)...
155                     - Qtnk(n) - sum(Losses)) <= sum(Movable_n))) ...
156                     & (max(FQ2 + FQ1) <= Q_S)) & (strcmp(input_format,'day')
                            ...
157                     | ((sum(Variables(:,1)) > Qmax & min(Qtnk)...
158                     < 0.001) | sum(Variables(:,1)) <= Qmax))
159             f = false;
160         elseif ((Qtnk_start + sum(FQ1) - Qtnk(n) - sum(Losses)) > (sum(Movable_n
                )...
161                 - 0.001)) & (Q_S < max(Variables(:,1))*2)
162             Q_S = Q_S * 0.98;
163         elseif (((Qtnk_start + sum(FQ1) - Qtnk(n) - sum(Losses)) < (sum(
```

```
                Movable_n))) |...
164                 ( Q_S < max(Variables(:,1))*2)) & Q_S < 10000
165                 Q_S = Q_S * 1.01;
166             else
167                 disp('error')
168                 disp(Z)
169                 f = false;
170             end
171         end
172
173         Qtnk = Qtnk';
174         FQ1 = FQ1';
175         FQ2 = FQ2';
176         Losses = Losses';
177         Delta_Qtnk = Delta_Qtnk';
178
179         Temp_result = table(Qtnk, FQ1+FQ2, FQ1, FQ2, Variables(:,1), Delta_Qtnk,...
180             Variables(:,2), Losses, 'VariableNames', {'Qtnk', 'FQ', 'FQ1', 'FQ2'...
181             ,'Load','Delta_tank', 'Temperature','Losses'});
182         Output(Z).Result = Temp_result;
183         Output(Z).Balance = (sum(FQ1) + sum(FQ2)) + Qtnk_start - Qtnk(n)...
184             - sum(Variables(:,1)) - sum(Losses);
185         Output(Z).Season = table2array(values((24*Z),8));
186         Output(Z).Q_S = Q_S;
187         Output(Z).Qtnk_strt = Qtnk_start;
188     end
189
190     Days = [(24.*eomday(2017,1:12)), (24.*eomday(2017,1:12))];
191     A = cumsum(Days);
192
193     Res = cat(1, Output.Result);
194     balance = cat(1, Output.Balance);
195
196     DeltaT(DeltaT==0) = NaN;
197
198     Vol = (3.13*3600)./(rho.*C_P.*DeltaT)';
199
200     Vol(isnan(Vol)) = 0;
201     DeltaT(isnan(Vol)) = 0;
202
203     x = find(table2array(values(:,8))==0);
204     Vol(x) = 0;
```

```
Result = cell(1,24);

Eta = (sum((table2array(Res(:,5))))-sum(table2array(Res(:,4)))-Qtnk(n))/(sum(
    table2array(Res(:,3))));

for L= 1:24
    if L == 1
        k = 1;
        l = A(1);
    else
        k = A(L-1)+1;
        l = A(L);
    end
    Result{1,L} = Res(k:l,:);
    Result{1,L}(:,8) = values(k:l,8);
    Result{1,L}(:,9) = values(k:l,8);
    Result{1,L}(:,10) = table(timestamp(k:l));

    if table2array(Result{1,L}(1,8)) == 1
        Basis = W;
    else
        Basis = S;
    end
    FQmax = max(table2array(Result{1,L}(:,2)));
    maxLoad = max(table2array(Result{1,L}(:,5)));
    Prices
end

P_en = (ELs + 0.2648 - Vol) * (table2array(Res(:,2)));
Pre_en = (ELs + 0.2648 - Vol) * table2array(values(:,6));

Price = P_en + sum(P_eff);
Price_pre = Pre_en + sum(Pre_eff);
diff = Price_pre - Price;

sum(counter >= Counter)
finn=find(counter>=Counter);
if Graphs == 1
    Plots
    ET_ver2
end

```

```
246 toc
247 P_eff = sum(P_eff);
248 Pre_eff = sum(Pre_eff);
249 % clearvars -except Price Price_pre Pre_eff Pre_en Output diff balance ...
250 %       counter Result Res Result_sorted Losses P_en P_eff
```

D MATLAB code to calculate the costs

```
%% Calculates the price based on the season.
% Separates into energy and power price and later adds them together.

if FQmax <= 200
    P_eff(L) = (FQmax)*Basis(1);
elseif FQmax > 200 && FQmax <= 500
    P_eff(L) = (FQmax-200) * Basis(2) + 200*Basis(1);
elseif FQmax > 500 && FQmax <= 800
    P_eff(L) = (FQmax-500) * Basis(3) + 300*Basis(2) + 200*Basis(1);
else
    P_eff(L) = (FQmax-800) * Basis(4) + 300*Basis(3) + 300*Basis(2)...
        + 200*Basis(1);
end

if maxLoad <= 200
    Pre_eff(L) = (maxLoad)*Basis(1);
elseif maxLoad > 200 && maxLoad <= 500
    Pre_eff(L) = (maxLoad - 200)*Basis(2) + 200*Basis(1);
elseif maxLoad > 500 && maxLoad <= 800
    Pre_eff(L) = (maxLoad - 500)*Basis(3) + 300*Basis(2) + 200*Basis(1);
else
    Pre_eff(L)=(maxLoad - 800)*Basis(4) + 300*Basis(3) + 300*Basis(2)...
        + 200*Basis(1);
end
```

E MATLAB code for the genetic algorithm

```
% This package is needed to run the program:
% https://www.mathworks.com/matlabcentral/fileexchange/39113-floating-point-
    number-conversion

clear, clc
tic

% Duration of simulation, in hours. Set to 0 if you use maxround
duration = 0;

% Maximum generations allowed. Set to 0 if you use duration
maxround = 1500;
number_of_chromosomes = 20;
p_c = 0.35;                 % p_c is the rate at which crossing happens
p_m = 0.01;                 % p_m is the mutation rate
input_format = 'day';       % Must be either week or day
precision = 3;

%% gathers data

Genetic_algorithm_allocation

if strcmp(input_format,'day') == true
    load Output_ver2_dag.mat
else
    load Output_ver2_week.mat
end
Liste_inp = round(QS1,precision);

%% Generates random input

for k = 1:number_of_chromosomes
    if k == 1
        Randominput = Liste_inp; % keeps original input
    else
        Randominput = round((0.7 + (1.3-0.7).*rand(1,1)).*Liste_inp,precision);
    end
    for i = 1:length(Randominput)
        [heig,leng] = size(Randominput(i));
        Parents{k,1}{i,1:length(Randominput(1,1:leng))} = float2bin(Randominput(
```

```
            i));
    end
end

%% Execution

if strcmp(input_format,'day') == true
    Ant = 730;
elseif strcmp(input_format,'week') == true
    Ant = 105;
else
    disp('input_format must be either week or day');
end

f = true;
roundcount = 0;
s = true;

while f
    roundcount = roundcount + 1;
    for Q = 1:length(Parents)
        clear Liste heig leng
        for k = 1:Ant
            if roundcount == 1
                phenotype{roundcount,Q}(k,1) = bin2float(char(Parents{Q,1}(k,1))
                    );
            else
                phenotype{roundcount,Q}(k,1) = bin2float(char(offspring{(
                    roundcount-1),Q}(k,1)));
            end
        end
        Q_S = phenotype{roundcount,Q}';
        val_max = max(Q_S);
        val_min = min(Q_S);
        if val_max >= 750 || val_min < 0
            flag = 1;
        else
            flag = 0;
        end
        Systemsimulering_rammeverk_ver2_tilpasset_gen_al
        Prisdiff{roundcount,1}(Q,1) = diff;
        Prisdiff{roundcount,1}(Q,2) = Q;
```

```
79          Prisdiff{roundcount,1}(Q,3) = flag;
80      end
81
82  %% Choosing parents
83
84      x = find(Prisdiff{roundcount,1}(:,1) <= 0);
85      Prisdiff{roundcount,1}(x,1) = 0;
86      x = find(Prisdiff{roundcount,1}(:,3) > 0);
87      Prisdiff{roundcount,1}(x,1) = 0;
88      P_k = Prisdiff{roundcount,1}(:,1)./sum(Prisdiff{roundcount,1}(:,1),'omitnan'
            );
89      q_k = cumsum(P_k,'omitnan');
90      r_k = rand(1,number_of_chromosomes);
91      X = find(r_k < p_c);
92      Len = length(X);
93      X(1,(length(X)+1):length(q_k)) = 0;
94
95      R = rand(length(q_k),1);
96
97      place(1) = 0;
98
99      I = 1;
100     y = 0;
101     z = 0;
102     for i = 1:length(q_k)
103         place(i,roundcount) = find(R(i)<=q_k,1);
104         if roundcount == 1
105             offspring{roundcount,i} = Parents{place(i,roundcount),1};
106         else
107             offspring{roundcount,i} = offspring{(roundcount-1),place(i,
                    roundcount)};
108         end
109         if X(I) == i
110             if rem(I,2) ~= 0
111                 y = y + 1;
112                 crossover{1,y} = offspring{roundcount,i};
113             else
114                 z = z + 1;
115                 crossover{2,z} = offspring{roundcount,i};
116             end
117             I = I + 1;
118         end
```

```
119     end
120
121 %% Crossing of parents
122
123     if rem(Len,2) ~= 0
124         Len = Len - 1;
125     end
126     a = randi((length(Q_S)-1),Len/2);
127     for i = 1:(Len/2)
128         [heig1, leng1] = size(crossover{1,i});
129         [heig2, leng2] = size(crossover{2,i});
130         part1 = crossover{1,i}(1:(a(i)),1:leng1);
131         part2 = crossover{2,i}((a(i)+1):length(Q_S),1:leng2);
132         offspring{roundcount,X(i)} = [part1;part2];
133     end
134
135 %% mutation of parents
136
137     for i = 1:number_of_chromosomes
138         leng = length(char(offspring{roundcount,i}(1,1)));
139         A = rand(1,Ant);
140         B = rand(1,leng)';
141         r_g = A.*B;
142         [row,col] = find(r_g < p_m);
143         for j = length(col)
144             placeholder = char(offspring{roundcount,i}(col(j)));
145             placeholder(row(j)) = char('0'+'1'-placeholder(row(j)));
146             offspring{roundcount,i}(col(j)) = cellstr(placeholder);
147         end
148         for k = 1:Ant
149             offspring_numeric{roundcount,i}(k,1) = bin2float(char(offspring{
                    roundcount,i}(k,1)));
150         end
151     end
152     Time = toc/3600;
153     if (roundcount >= maxround && duration == 0) || (Time >= duration &&
            maxround == 0)
154         f = false;
155     end
156 end
157
158 %% results
```

```
159
160 for k = 1:numel(Prisdiff)
161     [val(k),loc(k)] = max(Prisdiff{k,1}(:,1));
162 end
163 [global_max,Generation] = max(val)
164 Best_chromosome = loc(Generation)
165
166 toc
```

F A selection of monthly plots

F.1 Case A: March 2018

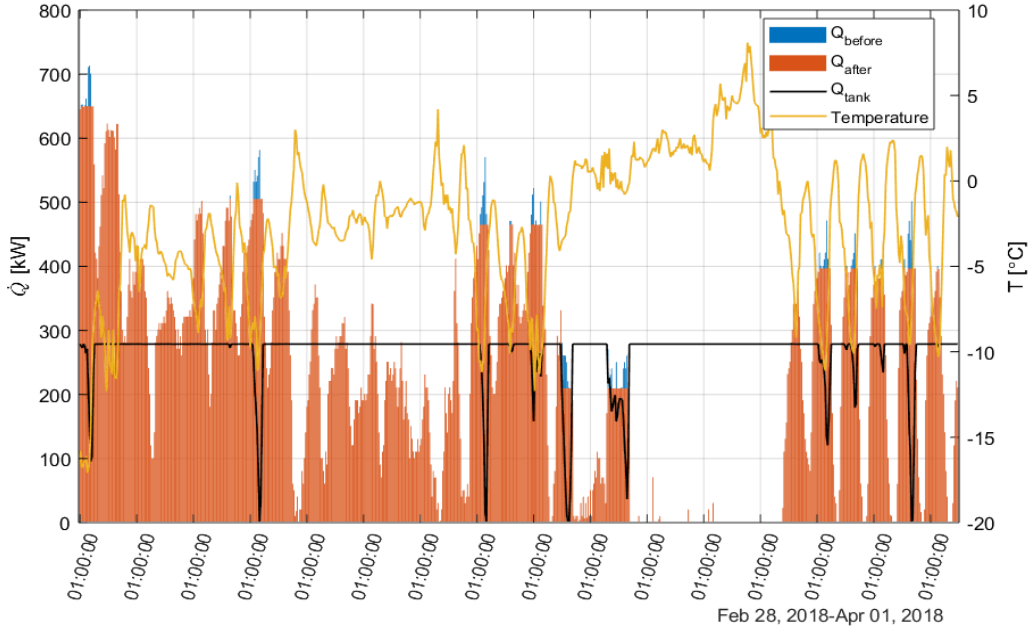

F.2 Case A: August 2018

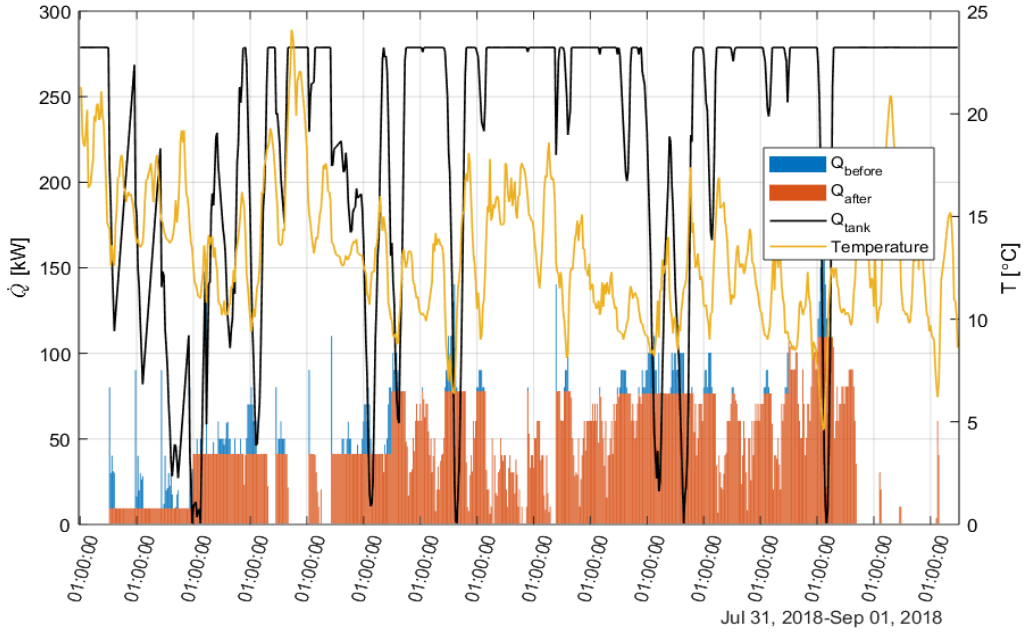

F.3 Case A:September 2018

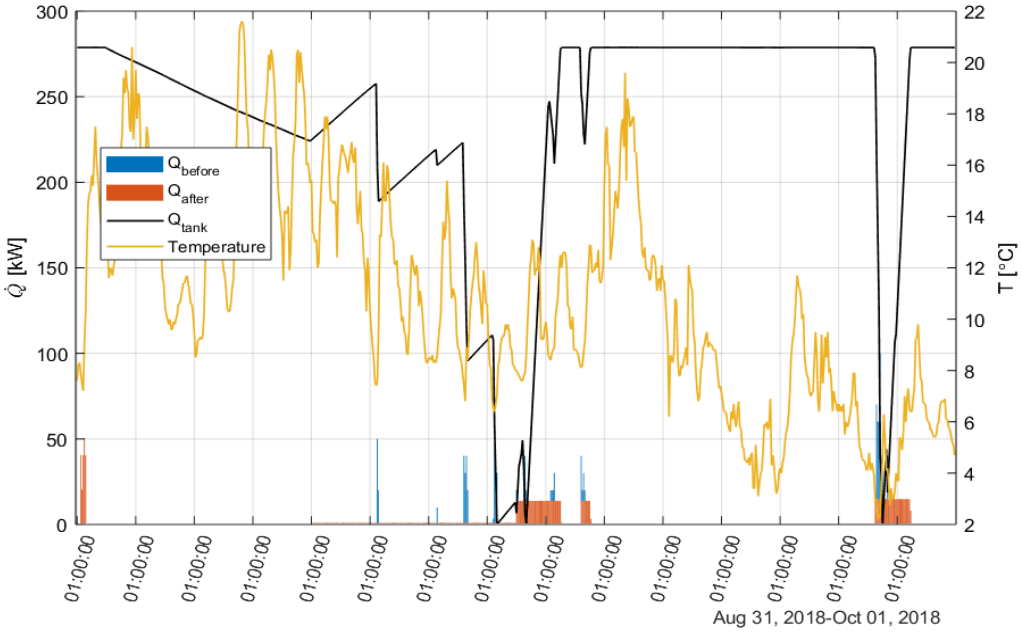

F.4 July 2018, 7m^3

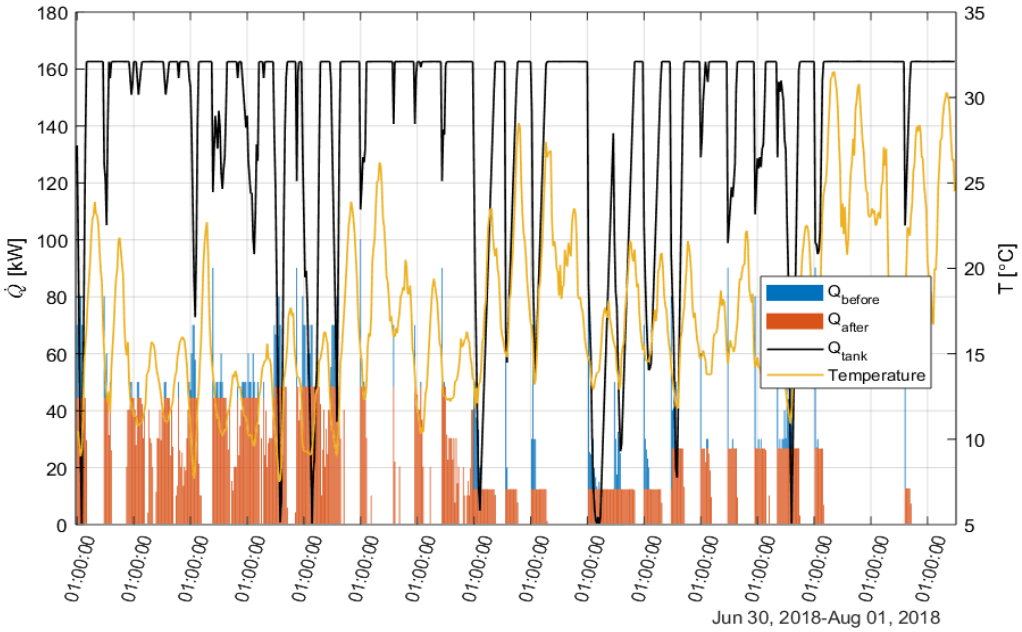

F.5 July 2018, 12m^3

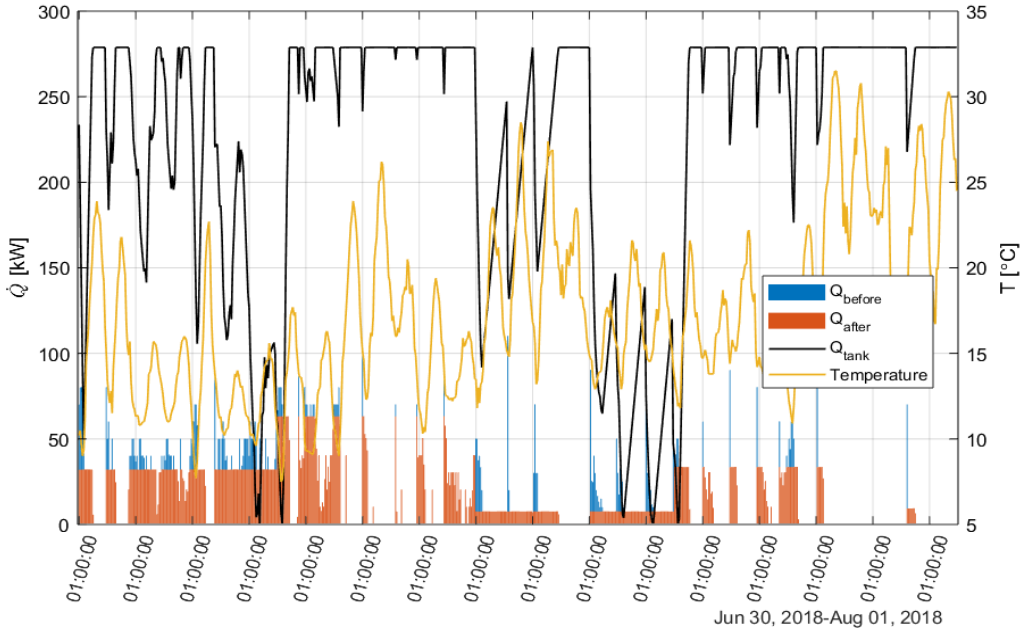

F.6 July 2018, 22m^3